

MASTER DEGREE IN CLINICAL AND FORENSIC ANALYTICAL TOXICOLOGY

CLINICAL TOXICOLOGY

Evaluation of P-glycoprotein expression/activity in HK2 cells

Jéssica Patrícia Veiga Matos

M

2020

Evaluation of P-glycoprotein expression/activity in HK2 cells

Jéssica Patrícia Veiga Matos

Faculdade de Farmácia



EVALUATION OF P-GLYCOPROTEIN EXPRESSION/ACTIVITY IN HK2 CELLS

Jéssica Patrícia Veiga Matos

Dissertation presented to the Faculty of Pharmacy of the University of Porto to fulfill the requirements necessary to obtain the Master's Degree in Clinical and Forensic Analytical Toxicology under the orientation of Professor Doctor Marta Prieto Vicente and Professor Doctor Ana I. Morales Martín and co-orientation of Professor Doctor Fernando Remião

Porto, October 2020

**DE ACORDO COM A LEGISLAÇÃO EM VIGOR, NÃO É PERMITIDA A REPRODUÇÃO
DE QUALQUER PARTE DESTA DISSERTAÇÃO.**

**IN ACCORDANCE WITH THE APPLICABLE LAW, IT IS NOT ALLOWED TO
REPRODUCE ANY PART OF THIS DISSERTATION.**

ACKNOWLEDGMENTS

The realization of this experimental work counted on several supports and incentives. Therefore, I would like to thank the participation and affection of several people.

I would like to begin by thanking Professor Doctor Marta Prieto Vicente for all the help and support of laboratory work development during this year.

To Professor Doctor Ana Isabel Morales, thanks for all the valuable suggestions and rectifications.

To Professor Doctor Fernando Remião, I would like to thank you for the availability and all the suggestions that showed all your knowledge.

To Renata Silva, thank you for all the knowledge about this area and for all the help you have provided.

Still in the professional forum, I would like to thank Dani, a colleague from laboratory, for all the knowledge transmitted and for the laboratory help in which he always assisted me with the greatest sympathy.

In general, thank everyone from TRECARD, especially at the Toxicology Laboratory, Laura and Alfredo, and also from the Cell Culture Laboratory, Anna and Claudia, who received me so kindly.

On a personal level, I would like to thank my family, especially my mother, Manuela Veiga, and my godmother, Elisa Veiga, for all the love and votes of confidence that they have given me in this last year.

To my boyfriend, Hélder Dias, thank you so much for your tireless presence (even if by video calls) and words of support and encouragement.

To all my friends, specially Elisabete Coelho, Diana Ribeiro, Tony Cardoso, Joana Couto and Sandra Sousa, thank you for all the time and words (and video calls) of affection you have given me during this phase.

The work was supported by UIDB/04378/2020 with funding from FCT/MCTES through national funds.



**VNIVERSIDAD
DSALAMANCA**
CAMPUS DE EXCELENCIA INTERNACIONAL



RESUMO

A glicoproteína-P (P-gp), expressa pelo gene *MDR1/ABCB1* no ser humano, é um transportador membranar de efluxo, incluído na superfamília “*ATP-binding cassette*” (ABC), largamente estudado pela sua capacidade de eliminação de tóxicos e fármacos a nível celular, de tecidos ou mesmo do organismo. Neste âmbito tem sido recentemente proposto que a modulação da P-gp pode constituir-se como estratégia terapêutica, uma vez que a sua ativação/indução reduz a acumulação intracelular dos seus substratos e, consequentemente, poderá levar a uma diminuição na citotoxicidade causada por eventuais agentes tóxicos. Neste contexto, o trabalho desenvolvido teve como objetivo avaliar se é possível reduzir a nefrotoxicidade de substratos da P-gp, modelando a sua expressão e/ou atividade nas células tubulares. Como resultados, confirmou-se a presença de P-gp nas células HK2 (“*human kidney 2*”), utilizando a técnica de Western Blotting, e caracterizou-se o perfil de citotoxicidade dos compostos em estudo doxorrubicina (DOX), rifampicina (RIF), tioxantona 5 (TX5) e zosuquidar (ZOS), após 24 h de exposição, por ensaios de MTT (brometo de 3-(4,5-dimetil-2-tiazolil)-2,5-difenil-2H-tetrazólio). De seguida, a atividade da P-gp, nas células HK2, foi avaliada após um período curto (30 min) ou longo (24, 48 e 72 h) de exposição a diferentes moduladores da P-gp, nomeadamente DOX (2 µM), RIF (20 µM) e TX5 (20 µM) como potenciais ativadores/indutores da P-gp; ZOS (1 µM) como inibidor específico da P-gp; e rodamina 123 (RHO 123; 10 µM) como seu substrato fluorescente. Por fim, as células HK2 foram expostas à cisplatina (CP; 10, 30 e 300 µM), fármaco nefrotóxico substrato da P-gp, na presença ou ausência de DOX, RIF, TX5 e ZOS, e a viabilidade celular (% de controlo) foi determinada por ensaios de MTT. Nos ensaios de exposição à TX5 observou-se a ativação da P-gp (aumento significativo na atividade da P-gp, após curto período de incubação), demonstrada pela diminuição na acumulação intracelular de RHO 123. Nos ensaios de RHO 123 com longos períodos de incubação, todos os compostos estudados foram capazes de aumentar significativamente a atividade da P-gp, possivelmente por fenómenos de indução, em todos os tempos estudados. Os ensaios de citotoxicidade realizados com cisplatina, na presença ou ausência dos possíveis ativadores/indutores, demonstraram que o RIF teve um papel importante na proteção das células HK2 contra a nefrotoxicidade induzida pela cisplatina. No entanto, alguns estudos adicionais com diferentes concentrações e tempos de incubação dos moduladores da P-gp, incluindo o ZOS, inibidor específico da P-gp, devem ser realizados para confirmar o papel da P-gp na diminuição da nefrotoxicidade induzida pela cisplatina nas células HK2.

Palavras chave: Glicoproteína P; Indução; Ativação; Doxorrubicina; Rifampicina; Tioxantonas; Cisplatina

ABSTRACT

P-glycoprotein (P-gp), expressed by the *MDR1/ABCB1* gene in humans, is an efflux membrane transporter, included in the “ATP-binding cassette” (ABC) superfamily, widely studied for its ability to eliminate toxic and drugs at the cellular level, tissues or even organism. In this scope, it has recently been proposed that the modulation of P-gp may constitute a therapeutic strategy, since its activation/induction reduces the intracellular accumulation of its substrates and, consequently, may lead to a decrease in cytotoxicity caused by possible toxic agents. In this context, the work developed aimed to evaluate whether it is possible to reduce the nephrotoxicity of P-gp substrates, modeling its expression and/or activity in the tubular cells. As a result, the presence of P-gp in HK2 cells (“human kidney 2”) was confirmed, using the Western Blotting technique, and the cytotoxicity profile of the compounds under study (doxorubicin (DOX), rifampin (RIF) was characterized), thioxanthone 5 (TX5) and zosuquidar (ZOS), after 24 h of exposure, by MTT assays (3-(4,5-dimethyl-2-thiazolyl)-2,5-diphenyl-2H-tetrazolium bromide). Then, P-gp activity in HK2 cells was evaluated after a short (30 min) or long (24, 48 and 72 h) period of exposure to different P-gp modulators, namely DOX (2 μ M), RIF (20 μ M) and TX5 (20 μ M) as potential activators/inductors of P-gp; ZOS (1 μ M) as a specific inhibitor of P-gp; and using rhodamine 123 (RHO 123; 10 μ M) as its fluorescent substrate. Finally, HK2 cells were exposed to cisplatin (CP; 10, 30 and 300 μ M), a nephrotoxic drug substrate for P-gp, in the presence or absence of DOX, RIF, TX5 and ZOS, and cell viability (% of control) was determined by MTT assays. In the TX5 exposure assays, P-gp activation was observed (significant increase in P-gp activity after a short incubation period), demonstrated by the decrease in the intracellular accumulation of RHO 123. In the RHO 123 assays with long periods of incubation, all studied compounds were able to significantly increase P-gp activity, possibly due to induction phenomena, at all times studied. Cytotoxicity tests performed with cisplatin, in the presence or absence of possible activators/inducers, demonstrated that RIF played an important role in protecting HK2 cells against cisplatin-induced nephrotoxicity. However, some additional studies with different concentrations and incubation times for P-gp modulators, including ZOS, a specific P-gp inhibitor, should be performed to confirm the role of P-gp in decreasing cisplatin-induced nephrotoxicity in HK2 cells.

Keywords: P-glycoprotein; Induction; Activation; Doxorubicin; Rifampicin; Thioxanthenes; Cisplatin

INDEX

ACKNOWLEDGMENTS.....	iii
RESUMO.....	iv
ABSTRACT	vi
INDEX	vii
FIGURES INDEX.....	ix
TABLES INDEX.....	xiii
LIST OF ABBREVIATIONS AND SYMBOLS	xiv
1. INTRODUCTION.....	1
1.1. Renal transporters	2
1.1.1. P-glycoprotein.....	6
1.1.2. P-gp inhibition, induction, and activation.....	10
1.2. Nephrotoxic agents.....	15
1.2.1. Cisplatin.....	18
1.3. Aims.....	20
2. MATERIAL AND METHODS.....	21
2.1. Materials.....	21
2.2. HK2 cells culture	21
2.3. P-glycoprotein expression in HK2 cells.....	23
2.4. Cytotoxicity essays.....	24
2.5. Evaluation of P-glycoprotein transport activity	26
2.5.1. RHO 123 efflux assay in cells pre-exposed for 30 minutes.....	26
2.5.2. RHO 123 efflux assay with pre-exposition for 24, 48 and 72 hours.....	27
2.6. Cisplatin-induced cytotoxicity assays	28
2.7. Statistical analysis	29
3. RESULTS AND DISCUSSION	30
3.1. P-glycoprotein expression on HK2 cells.....	30

3.2.	Cytotoxicity assays.....	31
3.3.	Evaluation of P-glycoprotein transport activity	34
3.4.	Cisplatin-induced cytotoxicity assays	39
4.	FINAL CONSIDERATIONS	46
5.	REFERENCES	47

FIGURES INDEX

Figure 1. Representative scheme of the renal excretion of the xenobiotics. Adapted from (Veiga-Matos et al. 2020).	1
Figure 2. Molecule movement in a given cell, including the phase 0 - III. Taken from (Veiga-Matos et al. 2020)	2
Figure 3. Schematic representation of the location and transport direction of the renal transporters. Adapted from (Veiga-Matos et al. 2020).	3
Figure 4. Representative scheme of the constitution of an ABC full-transporter, with two transmembrane domains (TMD) (with six transmembrane helices (TMH) each) and two nucleotide binding domains (NBD). Taken from (Veiga-Matos et al. 2020).	7
Figure 5. X-ray crystallography structure for P-gp with the NBDs are separated in varying degrees (A) and conformation changes resulting in extrusion of a substrate to the extracellular space (B). P-gp is represented as pink and ATP as yellow. Adapted from (Wessler et al. 2013; Waghray and Zhang 2018).	8
Figure 6. Representative scheme of the cells with normal, inhibited or induced/activated efflux transporters.	11
Figure 7. Chemical structure of zosuquidar (ZOS; IUPAC name: (2R)-1-[4-[(2S,4R)-3,3-difluoro-11-tetracyclo[10.4.0.0.2,4.0.5,10]hexadeca-1(16),5,7,9,12,14-hexaenyl]piperazin-1-yl]-3-quinolin-5-yloxypropan-2-ol), doxorubicin (DOX; IUPAC name: (7S,9S)-7-[(2R,4S,5S,6S)-4-amino-5-hydroxy-6-methyloxan-2-yl]oxy-6,9,11-trihydroxy-9-(2-hydroxyacetyl)-4-methoxy-8,10-dihydro-7H-tetracene-5,12-dione), rifampicin (RIF; IUPAC name: [(7S,9E,11S,12R,13S,14R,15R,16R,17S,18S,19E,21Z)-2,15,17,27,29-pentahydroxy-11-methoxy-3,7,12,14,16,18,22-heptamethyl-26-[(E)-(4-methylpiperazin-1-yl)iminomethyl]-6,23-dioxo-8,30-dioxa-24-azatetracyclo[23.3.1.1 ^{4,7} .0 ^{5,28}]triaconta-1(29),2,4,9,19,21,25,27-octane-13-yl] acetate) and thioxanthone 5 (TX5; IUPAC name: 2-isopropyl-9H-thioxanthen-9-one).	15
Figure 8. Cisplatin chemical structure.	18
Figure 9. Neubauer chamber. Numbers 1 - 5 represents the cells used to count HK2 cells.	22

Figure 10. Formula used to determine the number of cells in one microliter and, consequently, the volume to add to each well to obtain a given cell density and perform the following experiments.	23
Figure 11. Experimental design of zosuquidar (ZOS), thioxanthone 5 (TX5), rhodamine 123 (RHO 123), doxorubicin (DOX) and rifampicin (RIF) cytotoxicity experiments, by incubation for 24 h in HK2 cells.	25
Figure 12. Experimental design of the rhodamine 123 (RHO 123) efflux assays, with a 30-minutes exposure in HK2 cells to zosuquidar (ZOS; 1 μ M), thioxanthone 5 (TX5; 20 μ M), doxorubicin (DOX; 2 μ M) and rifampicin (RIF; 20 μ M).	26
Figure 13. Experimental design of the rhodamine 123 (RHO 123) efflux assays, with a 24, 48 and 72-hours HK2 cells exposure to thioxanthone 5 (TX5; 20 μ M), doxorubicin (DOX; 2 μ M) and rifampicin (RIF; 20 μ M).	27
Figure 14. Experimental design of the cisplatin cytotoxicity assays. Legend: CP. Cisplatin. Compound: doxorubicin (2 μ M), rifampicin (20 μ M), thioxanthone 5 (20 μ M) or zosuquidar (1 μ M).	28
Figure 15. Chemiluminescent image obtained in the membrane incubated with the primary antibody C219 mouse monoclonal anti-P-gp and the anti-mouse IgG-peroxidase secondary antibody. Red arrow represents the molecular weight of 170 kDa. Samples represented with green were obtained in the protein extraction from HK2 cells in culture medium with fetal bovine serum (FBS). Samples represented with orange were obtained in the protein extraction from HK2 cells in culture medium without FBS. To the samples represented in blue was added β -Mercaptoethanol.	30
Figure 16. Cell viability (% Control + DMSO) of HK2 cells exposed to different concentrations of zosuquidar, thioxanthone 5, rifampicin and doxorubicin, for 24 h, and rhodamine 123, for 2 h, based on the MTT assays. Data is presented as mean \pm standard error of 3 experiments with quadruplicates (n=12). Black line represents cell viability before treatment (time 0). *: p<0.05, **: p<0.01 and ***: p<0.001, compared with Control; #: p<0.05, ##: p<0.01 and ###: p<0.001, compared with Control + DMSO.	32
Figure 17. P-gp activity evaluated by fluorescence spectroscopy in HK2 cells through the rhodamine 123 accumulation assay performed in the presence of different ZOS concentrations (1, 2 and 5 μ M, for 30 min). Grey color represents control cells. Blue color represents the results obtained for ZOS-treated cells. Data is presented as mean \pm standard	

error of 3 experiments with triplicates (n=9). ***: p<0,001, compared with control. #: p<0.05, compared with 1 μ M ZOS..... 34

Figure 18. P-glycoprotein activity transport (% control) in HK2 cells exposed to thioxanthone 5 (TX5; 20 μ M; orange), doxorubicin (DOX; 2 μ M; red) and rifampicin (RIF; 20 μ M; yellow), for 30 min, based on RHO 123 assays. Grey color represents Control. Data is presented as mean \pm standard error of 3 experiments with triplicates (n=9). *: p<0.05 and ***: p<0.001, compared with control. 35

Figure 19. P-glycoprotein activity transport (% control) in HK2 cells exposed to thioxanthone 5 (TX5; 20 μ M), doxorubicin (DOX; 2 μ M) and rifampicin (RIF; 20 μ M), for 24 (blue), 48 (orange) and 72 h (green), based on RHO 123 assays. Data is presented as mean \pm standard error of 3 experiments with triplicates (n=9). *: p<0.05, **: p<0.01 and ***: p<0.001, compared with control. 36

Figure 20. Photos obtained from an optic microscope in the HK2 cells exposed to doxorubicin (DOX; 2 μ M), rifampicin (RIF; 20 μ M), thioxanthone 5 (TX5; 20 μ M) or zosuquidar (ZOS; 1 μ M) for 30 min, plus 18 h exposed to cisplatin (CP; 10 μ M, 30 μ M and 300 μ M) in the cisplatin-induced cytotoxicity assay. 39

Figure 21. Cell viability (%) of HK2 cells exposed to doxorubicin (DOX; 2 μ M), rifampicin (RIF; 20 μ M), thioxanthone 5 (TX5; 20 μ M) and zosuquidar (ZOS; 1 μ M) for 30 min, in the cisplatin-induced cytotoxicity assays, based on the MTT assays. Data is presented as mean \pm standard error of 3 experiments with quadruplicates (n=12). Black line represents cell viability before treatment (Time 0). *: p<0.5, **: p<0.01, and ***: p<0.001, compared with control; #: p<0.05, ##: p<0.01, ###: p<0.001, compared with control with DOX, RIF, TX5 or ZOS. 40

Figure 22. Photos obtained from an optic microscope in the HK2 cells exposed to doxorubicin (DOX; 2 μ M), rifampicin (RIF; 20 μ M) or thioxanthone 5 (TX5; 20 μ M) for 48 h, plus 18h exposed to cisplatin (CP; 10 μ M, 30 μ M and 300 μ M) in the cisplatin-induced cytotoxicity assay. 41

Figure 23. Cell viability (%) of HK2 cells exposed to doxorubicin (DOX; 2 μ M), rifampicin (RIF; 20 μ M), and thioxanthone 5 (TX5; 20 μ M), in the 48h cisplatin-induced cytotoxicity assays, based on the MTT assays. Data is presented as mean \pm standard error of 3 experiments with quadruplicates (n=12). Black line represents cell viability before treatment (Time 0). *: p<0.5, **: p<0.01, and ***: p<0.001, compared with control; ##: p<0.01, and ###: p<0.001, compared with control with DOX, RIF, TX5 or ZOS. 42

p<0.001, compared with control with DOX, RIF or TX5; β : p<0.05, $\beta\beta$: p<0.01, compared with CP10; α : p<0.05, compared with CP30. 42

Figure 24. Cell viability (%) of HK2 cells exposed to doxorubicin (DOX; 2 μ M), rifampicin (RIF; 20 μ M), and thioxanthone 5 (TX5; 20 μ M), in the 30 + 18 h cisplatin-induced cytotoxicity assays, based on the MTT assays. Data is presented as mean \pm standard error of 3 experiments with quadruplicates (n=12). Black line represents cell viability before treatment (Time 0). *: p<0.5, **: p<0.01, and ***: p<0.001, compared with control with control; #: p<0.5, ##: p<0.01, and ###: p<0.001, compared with DOX, RIF or TX5; $\beta\beta$: p<0.01, compared with CP10; $\alpha\alpha$: p<0.01, compared with CP30; \$\$: p<0.01, compared with CP300..... 43

TABLES INDEX

Table 1. Location and substrates of the main uptake transporters in proximal tubular cells. Adapted from (George et al. 2017; Ivanyuk et al. 2017; Shen et al. 2019; Veiga-Matos et al. 2020).....	4
Table 2. Location and substrates of the main efflux transporters in proximal tubular cells. Adapted from (George et al. 2017; Ivanyuk et al. 2017; Shen et al. 2019; Veiga-Matos et al. 2020).....	5
Table 3. Examples of P-gp inhibitors, inducers and/or activators. Adapted from (Balayssac et al. 2005; Palmeira et al. 2012; Silva et al. 2014, 2015b; Chufan et al. 2016; Alam et al. 2018; Elmeliegy et al. 2020a, b; Veiga-Matos et al. 2020).....	12
Table 4. Transporters and nephrotoxic agents which are transported by them.....	16

LIST OF ABBREVIATIONS AND SYMBOLS

Abbreviation	Connotation
ABC	ATP- binding cassette
ADME	Absorption, Distribution, Metabolism, Excretion - Toxicokinetics
AKI	Acute kidney injury
ATP	Adenosine triphosphate
BBB	Blood-brain-barrier
BCRP	Breast cancer resistance protein
BSA	Bovine serum albumin
cAMP	Cyclic adenosine monophosphate
CB	Cannabinoid receptor
CKD	Chronic kidney disease
CNS	Central nervous system
CP	Cisplatin
CTR	Copper transporter
DDI	Drug-drug interactions
DiBenzoRif	1,8-dibenzoyl-rifampicin
DMSO	Dimethyl sulfoxide
DNA	Deoxyribonucleic acid
DOX	Doxorubicin
EDTA	Ethylenediamine tetraacetic acid
ERK	Extracellular-signal-regulated kinase
FBS	Fetal bovine serum
FI	Fluorescence intensity
GNT	Phytoestrogen genistein
GSH	Glutathione
HBSS	Hanks' Balanced Salt solution
HIV	Human immunodeficiency virus
HK2	Human kidney 2
MATE	Multidrug and toxic extrusion
MDCK	Madin-Darby canine kidney
MDR	Multidrug resistance protein
MRP	Multidrug resistance-associated protein
MTT	3-(4,5-dimethylthiazol-2-yl)-2,5-diphenyl tetrazolium bromide
NBD	Nucleotide binding domain

NF- κ B	Nuclear factor kappa B
NRK-52E	Normal rat kidney epithelial
NSAIDs	Non-steroid anti-inflammatory drugs
OAT	Organic anions transporter
OATP	Organic anion transporting polypeptides
OCT	Organic cations transporter
OCTN	Organic carnitine/cations transporter
PAH	Polycyclic aromatic hydrocarbon
PBS	Phosphate-buffered saline solution
PEPT	Peptide transporter
P-gp	P-glycoprotein
PQ	Paraquat
QDs	Quantum dots
RedRif	Reduced rifampicin
RHO 123	Rhodamine 123
RIF	Rifampicin
SLC	Solute carrier
SNP	Single nucleotide polymorphism
URAT	Urate transporter
TCDD	Tetrachlorodibenzo-p-dioxin
TMD	Transmembrane domains
TMH	Transmembrane helices
TRECARD	Translational Research on Renal and Cardiovascular Diseases
TX5	Thioxanthone 5
VDR	Vitamin D receptor
WB	Western Blotting
ZOS	Zosuquidar

1. INTRODUCTION

Kidneys are the excretory organs of the human body making the excretion of various products of metabolism from the circulation and also of several xenobiotics that do not get transformed (George et al. 2017; Radi 2019). In this process, two steps occur: glomerular filtration, where ultrafiltrate is originated, and tubular secretion, where compounds are secreted into urine (Figure 1) (Robertson and Rankin 2006; George et al. 2017).

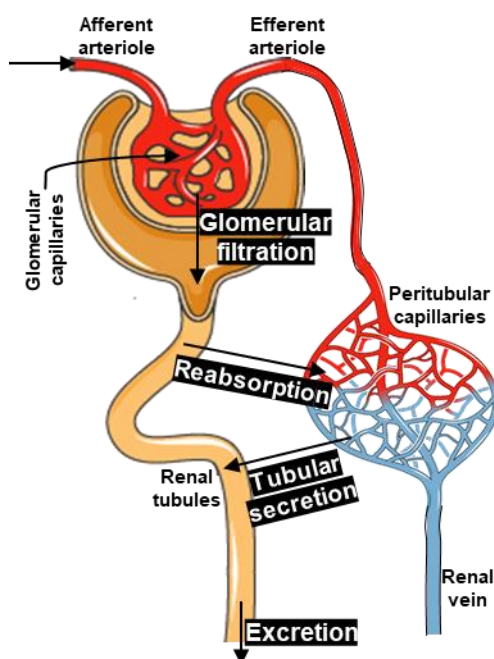


Figure 1. Representative scheme of the renal excretion of the xenobiotics. Adapted from (Veiga-Matos et al. 2020).

In the glomerulus the blood is filtered, entering by the afferent arteriole and exiting through the efferent arteriole. Renal function can be assessed by determining the glomerular filtration rate (Radi 2019). The compounds present in the ultrafiltrate are released into the urine or reabsorbed back into the bloodstream (Robertson and Rankin 2006; George et al. 2017). Thus, overall, the kidney retains essential nutrients (e.g., glucose, amino acids) and expels metabolic waste products (e.g., creatinine, uric acid) and xenobiotics (e.g., antiviral drugs and antibiotics) (Huo and Liu 2018). Tubular secretion is mostly performed in the proximal tubule (Aleksunes et al. 2008; George et al. 2017) and is carried out in two phases: (1) uptake of the compounds from the peritubular fluid into the tubular cell through the basolateral membrane and (2) efflux of these same compounds out of the cell into luminal fluid through the apical membrane (Robertson and Rankin 2006; Brown et al. 2008). The

majority of the molecules follow this path with the help of transporters present in the basolateral and apical membranes (Brown et al. 2008; George et al. 2017), and not by passive diffusion, since the molecules are very often hydrophilic as result of being charged at physiological pH. Thus, these transporters control the input and output molecules, being a key process for the physiology of tubular epithelial cells (Shen et al. 2019). By acting as gatekeepers, and given their interaction with xenobiotics, the transport mediated by these carriers is a totally different process from the passive process of glomerular filtration (Huo and Liu 2018).

1.1. Renal transporters

Transporters are large proteins incorporated into the cell membranes, which are expressed in several cells of the major organs with functions of absorption and elimination, such as liver, intestine, kidney, brain, tests and placenta, sites of high importance as regards the evaluation of the disposition of xenobiotics (DeGorter et al. 2012). These membrane proteins serve to control the uptake and efflux of the most varied molecules, from toxins to drugs and metabolites (Schlessinger et al. 2013). In fact, metabolism is often classified as phase I or II (functionalization or conjugation, respectively). More recently, the terms phase 0 and III have been associated with the uptake and efflux transport, respectively, thus characterizing the complete movement of a molecule in a given cell (Figure 2) (Döring and Petzinger 2014; Bush et al. 2017).

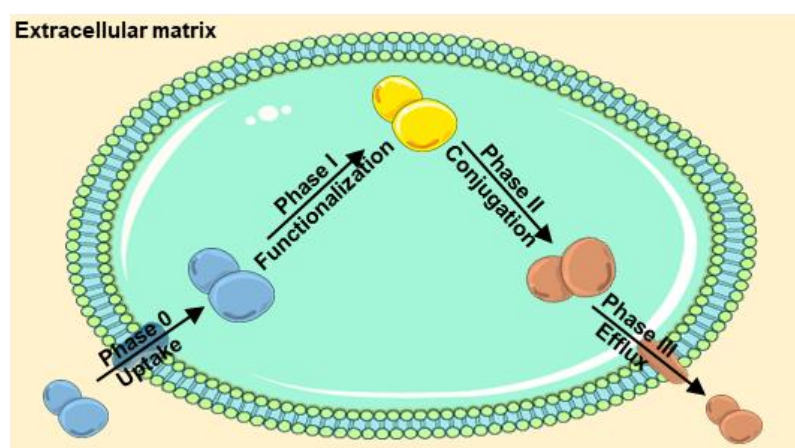


Figure 2. Molecule movement in a given cell, including the phase 0 - III. Taken from (Veiga-Matos et al. 2020)

Besides that major function, they also serve to regulate the movement of small endogenous molecules such as key metabolites, signaling molecules, vitamins, antioxidants (e.g., uric acid) and some hormones (Liu et al. 2016). In the kidneys, uptake transporters make the passage of the compounds from blood or ultrafiltrate into the proximal tubular cells while efflux transporters excrete them back into the blood or into the urine (Huo and Liu 2018). These transporters are expressed in greater amounts in the basolateral and apical membranes of the proximal tubular epithelial cells (Figure 3) (Ivanyuk et al. 2017).

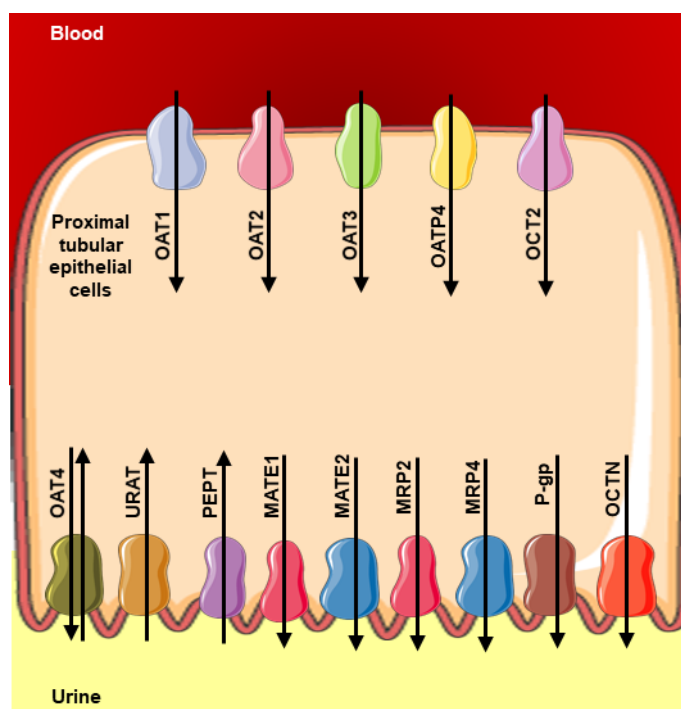


Figure 3. Schematic representation of the location and transport direction of the renal transporters. Adapted from (Veiga-Matos et al. 2020).

There are two super families that represents the most expressed transporters in the basolateral and apical membranes: the solute carrier (SLC) transporters superfamily (molecular weight of 40–90 kDa), which assure, mostly, the cellular uptake of the compounds from the blood at the basolateral membrane; and the adenosine triphosphate (ATP)-binding cassette (ABC) transporters superfamily (molecular weight of 140–180 kDa), which make the efflux to the tubular lumen on the opposite side of the cell, at the apical membrane (Schlessinger et al. 2013; Gameiro et al. 2017; Ivanyuk et al. 2017). In this way, it is important to note that the tubular secretion of a xenobiotic always involves at least one transporter of each type (Ivanyuk et al. 2017).

The SLC transporters are a large family of transmembrane proteins that share 20-25% of the homologous sequence (DeGorter et al. 2012), which includes more than 400 members grouped in 52 families, that perform various cellular functions cooperating with other proteins (Gameiro et al. 2017). This superfamily has members with high abundance in various organs (liver, kidney, blood-brain barrier) that have important functions in the toxicokinetics of their substrates (Klaassen and Lu 2008). The transport mechanisms used by transporters includes facilitated diffusion, ion coupling, and ion exchange, which are promoted by a gradient created by the ABC transporters (DeGorter et al. 2012). Table 1 shows the main uptake transporters and their respective characteristics, including the organic anions transporter (OAT), organic cations transporter (OCT), organic anion transporting polypeptides (OATP) and organic carnitine/cation transporters (OCTN).

Table 1. Location and substrates of the main uptake transporters in proximal tubular cells. Adapted from (Ivanyuk et al. 2017; George et al. 2017; Shen et al. 2019; Veiga-Matos et al. 2020).

Transporter	Gene	Location	Substrates
OAT1	<i>SLC22A6</i>	Basolateral membrane	PAH, antivirals, NSAIDs, antibiotics, diuretics, folate, α -ketoglutarate, cyclic nucleotides, prostaglandins, gut microbial metabolites, uremic toxins, vitamins, dietary compounds, uric acid, mercurial
OAT2	<i>SLC22A7</i>	Basolateral membrane	PAH, antivirals, salicylate, acetylsalicylate, prostaglandin E2, dicarboxylates, glutamate, uric acid
OAT3	<i>SLC22A8</i>	Basolateral membrane	Conjugated sex steroids, vitamins, aristolochic acid and other plant-derived metabolites (e.g., flavonoids), ochratoxin A, anti-viral, anti-cancer, antibiotics, anti-hypertensive, anti-inflammatory drugs
OAT4	<i>SLC22A11</i>	Apical membrane	Uric acid, diuretics, sulfated steroids, NSAIDs, antihypertensives, prostaglandins
URAT1	<i>SLC22A12</i>	Apical membrane	Uric acid
OCT2	<i>SLC22A2</i>	Basolateral membrane	Metformin, cisplatin, atenolol, histamine H2 blockers, HIV protease inhibitors, b-blockers, some platinum compounds, calcium channel blockers, antiarrhythmics, antimalarials, catecholamines, choline, acetylcholine, serotonin, creatinine
OATP4C1	<i>SLC04C1</i>	Basolateral membrane	Glycosides (digoxin and ouabain), thyroid hormones (triiodothyronine [T3] and thyroxine), cyclic adenosine monophosphate (cAMP), methotrexate, sitagliptin, estrone 3-sulfate, chenodeoxycholic acid, and glycocholic acid
OCTN1/2	<i>SLC22A4/5</i>	Apical membrane	valproic acid, cephaloride, ergothioneine, verapamil, quinidine and gabapentin

ABC superfamily include more than 100 transporters/channels that are prevalent in barrier organs, like intestine, liver, kidney, heart, lungs, brain (mainly in blood-brain-barrier (BBB)), placenta and testis. In human, 48 ABC transporters belonging to 7 families have been

identified, which have impact in the absorption, distribution, metabolism and excretion (ADME) of various endogenous and exogenous compounds and assure various physiological functions, like protection from toxic substances, metabolite transport and cell signaling (Gameiro et al. 2017; Gomez-Zepeda et al. 2019). These transporters, also called pumps, transport the molecules in only one direction (usually out of cells cytoplasm). Therefore, the movement is generally performed from the inner leaflet of the phospholipid bilayer to the outer leaflet or to an acceptor molecule, which results in cellular elimination towards various fluids, like feces, urine and bile (Silva et al. 2015b). In order to move the compounds across the cell membrane, ABC transporters need the energy obtained from the hydrolysis of ATP. Thus, these transmembrane proteins can export the compound reducing its cellular concentration. This process is called the primary active transport since, in addition to spending ATP, it is done against the concentration gradient (DeGorter et al. 2012; Döring and Petzinger 2014; Silva et al. 2015b). Table 2 shows the major efflux transporters and their respective characteristics, including member of this superfamily, between them: Multidrug resistance proteins (MRP); Multidrug resistance (MDR); Breast cancer resistance protein (BCRP); Multidrug and toxic extrusion (MATE).

Table 2. Location and substrates of the main efflux transporters in proximal tubular cells. Adapted from (Ivanyuk et al. 2017; George et al. 2017; Shen et al. 2019; Veiga-Matos et al. 2020)

Transporter	Gene	Location	Substrates
MRP1	<i>ABCC1</i>	Apical membrane	GSH, cysteinyl leukotrienes, glucuronide and sulfate conjugates, anthracyclines, Vinca alkaloids, and antivirals
MRP2	<i>ABCC2</i>	Apical membrane	GSH and glucuronide conjugates, leukotrienes, methotrexate, ochratoxin A
P-gp	<i>ABCB1</i>	Apical membrane	Anticancer agents, cardiac glycosides (digoxin), beta-adrenoreceptor antagonists, Ca ²⁺ channel blockers, HIV protease inhibitors, steroids, immunosuppressants, antiemetic drugs, antibiotics, antimicrobial, antiretrovirals, lipid lowering agents, histamine H ₁ - receptor antagonists, phenobarbital, phenytoin, others
BCRP	<i>ABCG2</i>	Apical membrane	Urate, cholesterol, plant sterols, phospholipids, chemotherapeutics, anthracycline drugs, nucleoside analogs, fluorophores, conjugated anions estrone3- sulfate, flavonoids, folates (folic acid), riboflavin (vitamin B12), porphyrins
MATE1	<i>SLC47A1</i>	Apical membrane	Histamine H ₂ receptor antagonist, cimetidine, the antidiabetic agent, metformin, and the herbicide, paraquat
MATE2-K	<i>SLC47A2</i>	Apical membrane	Metformin, cimetidine, antibiotics, oxaliplatin

In this work, from the mentioned efflux transporter, the MDR1 transporter, also known as P-glycoprotein, was the one studied and, therefore, it will be described in more detail in the following section.

1.1.1. P-glycoprotein

P-glycoprotein (P-gp), comes from “permeability-glycoprotein”, also called multidrug resistance 1 (MDR1), is expressed by the *MDR1/ABCB1* gene in humans and belongs to the superfamily of ABC transporters, as we already discuss (Balayssac et al. 2005; Callaghan et al. 2014). In 1976, Juliano and Ling discovered and isolated this protein from hamster ovary cells (Juliano and Ling 1976). Since then, P-gp has been a well-studied protein due to its particularly important role in protecting various sensitive tissues against different toxins, by actively pumping these molecules to outside of the cells and, consequently, decreasing their intracellular concentration. Thus, it has an important role in the process of protection and detoxification and in the phenomenon of multidrug resistance (MDR) in tumor chemotherapy (Balayssac et al. 2005; Martins et al. 2019). In humans, there are two P-gp: MDR1 and MDR3. However, only the coding product of the *MDR1/ABCB1* gene participates actively and significantly in the disposition of xenobiotics in various organs. The *MDR3* gene encodes for a phospholipid lipase protein, expressed exclusively on the canalicular domain of hepatocytes (Kim 2002). Thus, in this work we will always be referring only to MDR1. This transporter is synthesized in the endoplasmic reticulum as a glycosylated intermediate with a molecular weight of 150-170 kDa, being the carbohydrate moiety further modified in the Golgi apparatus prior to the export to the cell surface (Silva et al. 2015b; Leopoldo et al. 2019; Martins et al. 2019). Like others ABC transporters, P-gp owns two transmembrane domains (TMD) and two nucleotide domains (NBD), being considered a full transporter (Figure 4). In this way, the substrates of P-gp bind to a binding site intracellularly and, following the phosphorylation of the protein with ATP spending by hydrolysis, a flip-flop movement occurs in which the substrate is extruded to the luminal side. The return to the initial state of the protein takes place by dephosphorylation (Cascorbi 2011; Konieczna et al. 2011; Silva et al. 2015b; Martins et al. 2019).

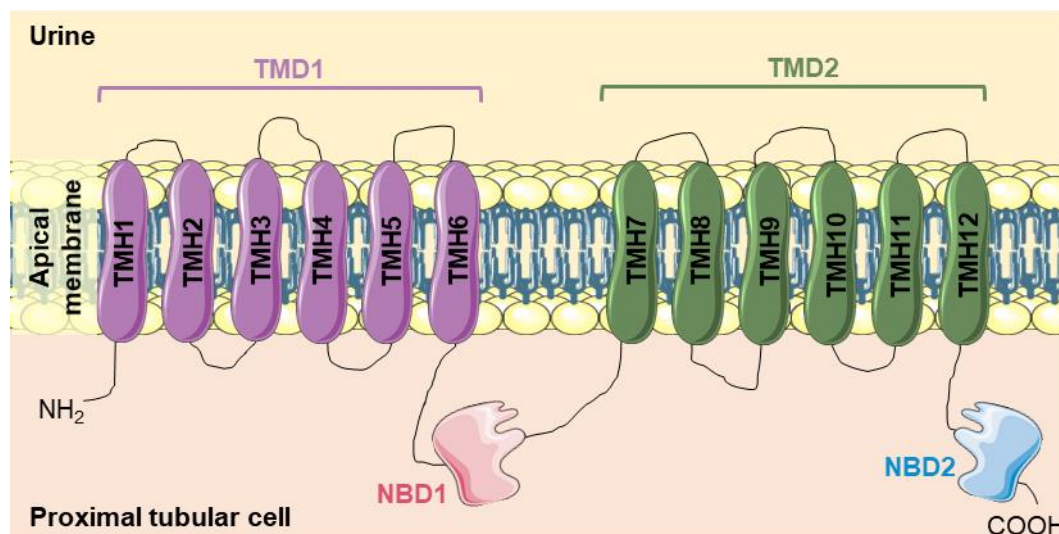


Figure 4. Representative scheme of the constitution of an ABC full-transporter, with two transmembrane domains (TMD) (with six transmembrane helices (TMH) each) and two nucleotide binding domains (NBD). Taken from (Veiga-Matos et al. 2020).

The structures obtained by X-rays from P-gp are inverted V-shaped formations, in which the two TMDs are crossed (together with TMH4/5 at TMD 1 and TMH10/11 at TMD 2) and the two NBDs are separated in varying degrees (Figure 5A). The drugs are believed to enter this cavity for connection through the open door to the cytoplasm and the internal membrane leaflet. This region includes several sites for phosphorylation, but with no defined role in the expression and transport of P-gp transported drugs. P-gp undergoes dynamic conformational changes through which drug binding sites alternately access the two sides of the membrane, connecting a charge on one side and releasing it on the other (Mollazadeh et al. 2018; Waghray and Zhang 2018). The membrane transporter work depends on the energy of the ATP hydrolysis. It is suggested that the binding of ATP to the NBD and the dimerization of the NBD are a driving force for this function. The hydrolysis energy causes complete conformational changes in the TMD and catalyzes the efflux of the substrate through the TMD and the lipid bilayer, and then there is a redefinition of the membrane transporter to its original conformation (Mollazadeh et al. 2018). Figure 5B shows the x-ray crystallography structure for P-gp, exemplifying ATP binding to produce conformation changes resulting in extrusion of a substrate to the extracellular space (Wessler et al. 2013; Waghray and Zhang 2018).

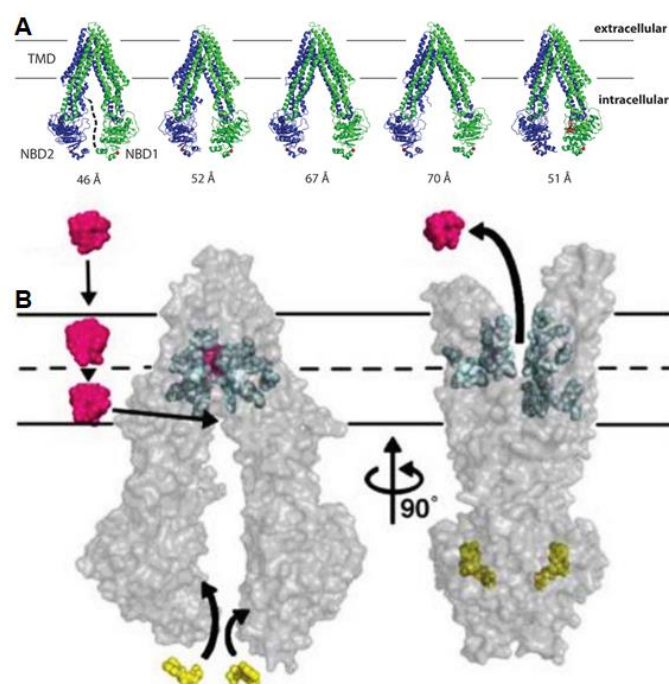


Figure 5. X-ray crystallography structure for P-gp with the NBDs are separated in varying degrees (A) and conformation changes resulting in extrusion of a substrate to the extracellular space (B). P-gp is represented as pink and ATP as yellow. Adapted from (Wessler et al. 2013; Waghray and Zhang 2018).

P-gp has low expression in most human tissues, but is found in much higher concentrations in epithelial cells of the intestine (apical zone of the lower gastrointestinal tract enterocyte - jejunum, duodenum, ileum and colon), limiting the absorption of drug substrates from the gastrointestinal tract; bile ducts of the liver and proximal kidney tubules, resulting in improved excretion of drug substrates in bile and urine, respectively; blood-brain barrier, limiting the entry into the central nervous system (CNS) of a variety of xenobiotics and/or their metabolites; hematopoietic cells (where its function remains unknown); and other sites, such as pancreatic ducts, adrenal gland, placenta, endometrium, testicles. P-gp expression and function at the kidney proximal tubules has been proved by using several *in vitro* models, per example, immortalized human proximal tubule cell lines, like HK2 cells (human kidney 2) (Tramonti et al. 2001), and immortalized epithelial cell lines isolated from rat kidney proximal tubule, as GERP cells (Masereeuw et al. 2010), and also by using 3D models of proximal tubules (Vormann et al. 2018). Furthermore, in general, its location reinforces the importance of its localization in the accomplishment of its function. Its physiological role of secreting endogenous and exogenous metabolites (through phase III-mediated transport) influences the toxicokinetics of several compounds (Kim 2002; Uchida et al. 2016; Leopoldo et al. 2019; Martins et al. 2019). This is what happens in so-called

"normal" cells, under physiological conditions. However, in tumor cells there is an overexpression of P-gp, which causes anticancer agents to be exported from the tumor cells. This phenomenon keeps the concentration of these drugs below the therapeutic threshold, which can lead to a sub-toxic effect on these cells, thus creating tumor resistance to these types of agents (Mollazadeh et al. 2018).

This transporter carries a wide variety of compounds, being a non-specific transporter. P-gp has some substrates in common with MRP1 and MRP2, more specifically cytostatic agents (Cascorbi 2011). The substrates of P-gp vary greatly in size, structure, and function, ranging from small molecules, such as organic cations, carbohydrates, amino acids, and some antibiotics, to macromolecules such as polysaccharides and proteins, which is according to the information that P-gp is a protective protein against various substances (Silva et al. 2015b). Several drugs are considered P-gp substrates, among them: anticancer agents, cardiac glycosides (e.g., digoxin), β -adreno receptor antagonists, Ca^{2+} channel blockers, HIV protease inhibitors, steroids, immunosuppressants, antiemetic drugs, antibiotics, antimicrobial, antiretrovirals, lipid lowering agents, histamine H1- receptor antagonists, phenobarbital, phenytoin, and many others (Döring and Petzinger 2014; Ivanyuk et al. 2017; George et al. 2017). Between them, some are particularly nephrotoxic, like levofloxacin, an antibiotic (Ramalakshmi et al. 2003); tenofovir, an antiviral (George et al. 2017); cisplatin, an anticancer agent (Silva et al. 2015b); cyclosporine A, an immunosuppressant (Kotowski et al. 2019); paraquat, an herbicide (Silva et al. 2014); and, even, arsenic, a metal (Orr and Bridges 2017).

Additionally, polymorphisms affecting the *MDR1/ABCB1* gene should also be considered. Indeed, *MDR1/ABCB1* polymorphisms are associated with lower digoxin renal clearance, modified efficacy and nephrotoxicity of chemotherapeutics, antivirals and immunosuppressants, like cyclosporine (due to impaired apical efflux) (Ivanyuk et al. 2017). In addition to these effects, *MDR1/ABCB1* polymorphisms can also contribute to the alteration of the drugs disposition and, consequently, to the interindividual variability in response to various drugs, like morphine and other opioids (e.g., methadone) (Ranzani et al. 2009). Some authors have been studying the polymorphisms of the P-gp coding gene. Hoffmeyer *et al* observed a significant correlation of a P-gp polymorphism (C3435T in exon 26) with its levels of expression and function. Individuals homozygous for this polymorphism [24% of the sample population (n = 5188)] had significantly lower duodenal P-gp expression and the highest digoxin plasma levels, suggesting that this polymorphism affects the absorption and tissue concentrations of numerous other P-gp substrates (Hoffmeyer et al. 2000). Saiz-Rodríguez *et al* also analyzed the C3435T polymorphism and observed that it can affect the elimination of some drugs in different ways. They observed enhanced

elimination of risperidone, trazodone and dehydro-aripiprazole, while in the case of olanzapine and citalopram a reduction in the elimination occurred. On the other side, there were no changes detected in quetiapine, aripiprazole, sertraline and agomelatine elimination (Saiz-Rodríguez et al. 2018). Kim *et al* carried out the polymorphism analysis from 37 healthy European American and 23 healthy African American subjects, identifying 10 single nucleotide polymorphisms (SNPs). Three SNPs (C1236T in exon 12; C3435T in exon 26; G2677T, Ala893Ser in exon 21) were found to be linked (*MDR1*2* allele, which is suggested to cause an enhanced P-gp activity) and occurred in 62% of European Americans and 13% of African Americans. *In vitro* experiments indicated an enhanced efflux of digoxin by cells expressing the *MDR1*-Ser893 variant. In humans, *MDR1*1* and *MDR1*2* variants were associated with differences in fexofenadine (a known substrate of P-gp) levels, consistent with the *in vitro* data, suggesting that, *in vivo*, P-gp activity among subjects with the *MDR1*2* allele is also enhanced (Kim et al. 2001).

1.1.2. P-gp inhibition, induction, and activation

Both in therapeutics and in cases of intoxication, multiple xenobiotics can be administered simultaneously, triggering drug-drug interactions (DDIs). DDIs may result in greater or lesser amounts of the xenobiotic, in the event of inhibition or induction/activation, respectively (Giacomini et al. 2010; Giacomini and Huang 2013). Inhibition can be competitive, where drugs compete for the same binding site to the carrier, binding to the one with the highest affinity; or non-competitive, where one of the drugs binds to a non-transporting site by altering the conformation of the protein (Ivanyuk et al. 2017). On the other hand, there are still compounds that increase the transport, which can occur by induction of *de novo* protein synthesis or directly by transporter activation. Inducers thus cause an increased expression of this transporter, causing a greater number of transporters available to carry out the substrates transport. Activators bind to the transporter, making it perform its work more efficiently, that is, the number of transporters is maintained but the substrate transport is increased (Silva et al. 2014, 2015a). In the therapeutics, compounds have been studied to inhibit or, alternatively, induce/activate the activity of these transporters, taking advantage of DDIs that may alter pharmacokinetics and pharmacodynamics of other compounds that are co-administered (König et al. 2013; Momper et al. 2019). P-gp, in the presence of inhibitors, will not perform its job effectively, leading to an accumulation of compounds intracellularly, which can be therapeutically useful to overcome the MDR phenomenon. However, in the presence of inducers or

activators P-gp will export compounds faster, leading to their faster urinary excretion, which can be a potential antidotal strategy in intoxication scenarios (Figure 6).

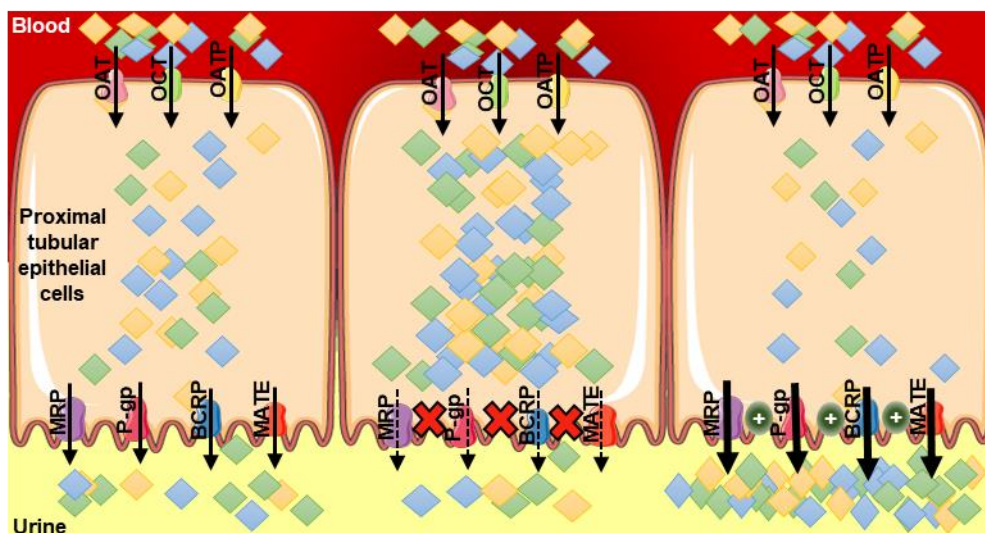


Figure 6. Representative scheme of the cells with normal, inhibited or induced/activated efflux transporters.

Noteworthy, P-gp expression and activity are frequently altered by their own substrates, which leads to consequent changes in their pharmacokinetics, bioavailability, toxicity, and therapeutic response, leading to DDIs among P-gp substrates (Wu et al. 2016). Table 3 presents some examples of P-gp substrates, inhibitors, inducers and activators, known in the literature.

The first studies carried out on this protein were due to its role in resistance to anticancer agents, being mainly focused on achieving the inhibition of P-gp as a therapeutic measure. In other words, the objective was to inhibit the export of anticancer agents from tumor cells, prolonging their effect. However, the presence of P-gp in other cells of the human body, other than tumor cells, made this inhibition strategy problematic because chemical inhibitors do not discriminate P-gp expressed at normal sites in the body from that found in cancerous tissue, leading to the accumulation of various toxics in different tissues of the human body (Callaghan et al. 2014; Lopes et al. 2018). Anyway, with these studies, it was possible to define several compounds as P-gp inhibitors. The mechanism of P-gp inhibition is thought to involve one of four pathways: direct inhibition of binding sites that block the transport of substrates (most frequent); ATP binding inhibition; ATP hydrolysis; coupling of ATP hydrolysis to the translocation of the substrate (Wessler et al. 2013).

Table 3. Examples of P-gp inhibitors, inducers and/or activators. Adapted from (Balayssac et al. 2005; Palmeira et al. 2012; Silva et al. 2014, 2015b; Chufan et al. 2016; Alam et al. 2018; Elmeliegy et al. 2020a, b; Veiga-Matos et al. 2020).

P-gp substrates	P-gp inhibitors	P-gp inducers	P-gp activators
<ul style="list-style-type: none"> ▪ Clarithromycin ▪ Cisplatin ▪ Cyclosporine A ▪ Berberine ▪ Dabigatran ▪ Digoxin ▪ Doxorubicin ▪ Eteclate ▪ Fexofenadine ▪ Hoechst- 33342 ▪ Irinotecan ▪ Loperamide ▪ Paclitaxel ▪ Quinidine ▪ Rhodamine 123 ▪ Ritonavir ▪ Talinolol ▪ Vinblastine 	<ul style="list-style-type: none"> ▪ Clarithromycin ▪ Elacridar ▪ Itraconazole ▪ Propafenone ▪ Quinidine ▪ Tariquidar ▪ Verapamil ▪ Zosuquidar 	<ul style="list-style-type: none"> ▪ Abacavir ▪ Aflatoxin B1 ▪ Amiodarone ▪ Atazanavir ▪ Benzo(a)pyrene ▪ Benzo(e)pyrene ▪ Bilirubin ▪ Bromocriptine ▪ Budesonide ▪ Cadmium chloride ▪ Caffeine ▪ Corticosterone ▪ Cyclophosphamide ▪ Cyclosporine A ▪ Curcumin ▪ Carbamazepine ▪ Dexamethasone ▪ Dehydroxylated xanthenes ▪ Doxorubicin ▪ Genistein ▪ Insulin ▪ Ivermectin ▪ Morphine ▪ Phenytoin ▪ Phenobarbital ▪ Probenecid ▪ Propranolol ▪ Quercetin ▪ Rifampin ▪ Ritonavir ▪ Rifabutin ▪ St. John's wort extract ▪ Talazoparib ▪ TCDD 	<ul style="list-style-type: none"> ▪ Di-hydroxylated xanthenes ▪ Rifampicin derivatives ▪ Thioxanthonic derivatives

In the present study, zosuquidar (ZOS; Figure 7) was used as a known P-gp inhibitor, since it has a greater inhibitory activity than other inhibitors such as tariquidar or elacridar (Mollazadeh et al. 2018). ZOS is a third generation P-gp inhibitor that also inhibits the basal ATP hydrolysis of P-gp (Chufan et al. 2016). It has been suggested by some authors that the transporter is in an occluded conformation with a central, enclosed, inhibitor-binding pocket lined by residues from all TMHs. The pockets almost swing the entire width of the lipid membrane and are occupied exclusively by two closely interacting zosuquidar molecules. These authors observed two main P-gp conformations, characterized by a distinct degree of NBD opening, but both conformations revealed bound to the zosuquidar

molecules (Alam et al. 2018, 2019). Due to its well-known P-gp inhibitory effect, it has also been used at the kidney level in several studies. Nies *et al* published a study where they generated a Madin-Darby canine kidney strain II (MDCKII) cell line stably expressing human *OCT1* together with human *MDR1*. This group used ZOS (1 and 5 μ M; 30 min) as a specific P-gp inhibitor, and it strongly inhibited berberine efflux into the apical compartment (Nies et al. 2008). Furthermore, Arakawa *et al* investigated the usefulness of kidney slices obtained from rats for the evaluation of influx and efflux transport in apical membrane, including P-gp activity. In the presence of ZOS (1 μ M; 5 and 15 min), these researchers observed an increased accumulation of a P-gp substrate, azasetron (Arakawa et al. 2019).

More recent studies have focused on the induction/activation of this pump to avoid the toxicity caused by some P-gp substrates, being proposed as a potential antidotal pathway. This is, the increase in P-gp expression/activity may be highlighted as a tissue protection strategy, by limiting the intracellular accumulation of its substrates and, consequently, reducing their toxicity. P-gp activators have the benefit of increasing P-gp activity without interfering with P-gp protein expression, being a rapid process when compared with the use of P-gp inducers (Lopes et al. 2018; Martins et al. 2019; Silva et al. 2020). To the best of our knowledge, studies about the P-gp induction or activation at the kidney level are scarce. Semeniuk et al evaluated the usefulness of phytoestrogen genistein (GNT) on P-gp expression in rat liver, kidney, and ileum. However, they observed that GNT (5 mg/kg/day for 3 consecutive days, subcutaneously, 24 h before the analysis) significantly increased hepatic P-gp expression and activity, but renal and intestinal P-gp levels remained unchanged (Semeniuk et al. 2020). In another study, researchers investigated if the increase in P-gp expression at the rat liver and kidney was caused by the vitamin D receptor (VDR), after treatment with dihydroxyvitamin D3 [1,25(OH)₂D3] (2.5 μ g/kg every other day for 8 days, intraperitoneally), the natural ligand of VDR. Renal and brain P-gp protein levels were significantly increased (3.45-fold), causing an increase in renal (74%) and total body (34%) clearances of digoxin (Chow et al. 2011).

Furthermore, although the studies concerning P-gp activation/induction at the kidney level are limited, several studies were carried out at the intestinal level aiming to propose the P-gp positive modulation as a therapeutic strategy. These studies showed that P-gp inducers, like doxorubicin (DOX), can significantly increase P-gp expression/activity in Caco-2 cells, leading to a more efficient transport of toxic substrates, like paraquat (PQ), to the extracellular matrix, resulting in a decreased PQ intracellular accumulation and, consequently, to a reduction in the cytotoxicity of the herbicide. Furthermore, Silva *et al* demonstrated a way to decrease the toxicity of PQ using di-hydroxylated xanthenes or thioxanthonic derivatives as P-gp inducers and/or activators (Silva et al. 2014, 2015a).

Lopes *et al* also successively characterized thioxanthonic derivatives, particularly chiral aminated thioxanthenes, as P-gp activators (Lopes *et al.* 2018). In fact, one of these thioxanthonic derivatives, TX5, was also tested in *ex vivo* and *in vivo* studies, where an increase in P-gp activity was observed in rat distal ileum after exposure to the thioxanthonic P-gp activator (Rocha-Pereira *et al.* 2020). More recently, oxygenated xanthenes were identified as potential P-gp inducers and activators at the intestinal level, by using the Caco-2 cells and SW480 cells as *in vitro* models (Martins *et al.* 2019; Silva *et al.* 2020).

There is evidence of the presence of this pump in other barriers with high importance, like the BBB, where it plays a physiological function of tissue protection by regulating the entrance of neurotoxins. Indeed, it seems that a connection between dysfunctional ABC transporters and neurological disorders exists. In that way, P-gp plays an essential role in many neuropathologies, by reducing drug efficacy (extruding therapeutic agents), and by being altered in CNS diseases, in what concerns to its expression and/or function. Noteworthy, dysfunction of ABC transporters, at the expression and/or activity level, has been associated with many neurological diseases, like Alzheimer's Disease; Amyotrophic lateral sclerosis; Brain Tumors; Creutzfeldt-Jakob's disease; Epilepsy; Human immunodeficiency virus (HIV) encephalopathy; Ischemic stroke/hypoxia; Mental disorders (depression and schizophrenia); Multiple Sclerosis; Parkinson's disease (Gil-Martins *et al.* 2020).

In the present study, we chose doxorubicin (DOX; Figure 7), rifampicin (RIF; Figure 7) and one thioxanthonic derivative (TX5; Figure 7) to be studied as inducers and activators of P-gp at the kidney level, aiming to reduce the toxicity of nephrotoxic agents. DOX is a cytotoxic antineoplastic antibiotic used in the therapy of several forms of lymphoma, leukemia, sarcoma and solid tumors (Pugazhendhi *et al.* 2018). The link between DOX and P-gp was identified as driven by electrostatic repulsion in the early stage and then followed by hydrophobic interaction in the later stage, based on an analysis of binding free energy between P-gp and doxorubicin (Wang *et al.* 2019). RIF was discovered in 1965 and it is valued for its sterilizing activity and ability to shorten treatment of tuberculosis (Grobbelaar *et al.* 2019). It has been shown that RIF is an inducer of P-gp by activating a nuclear receptor, the pregnane X receptor. Hasanuzzaman *et al* studied the effect of RIF on *MDR1/ABCB1* gene expression in THP1 macrophages, analyzing the intracellular concentration of protonamide in the presence of RIF (1×10^5 nM, 48 h). They observed that RIF-treated THP1 macrophages exhibited strong efflux of the P-gp substrate, resulting in a reduced intracellular concentration of rhodamine 123 (RHO 123) and protonamide (Hasanuzzaman *et al.* 2019).

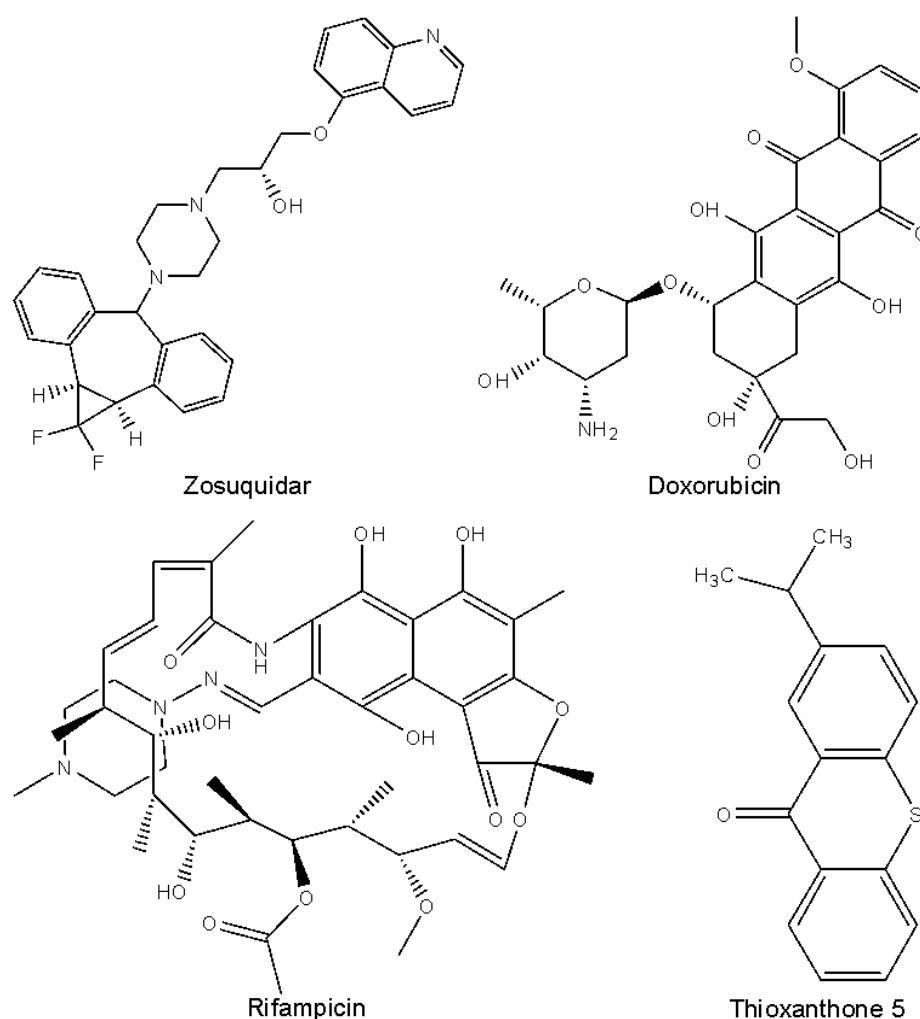


Figure 7. Chemical structure of zosuquidar (ZOS; IUPAC name: (2R)-1-[4-[(2S,4R)-3,3-difluoro-11-tetracyclo[10.4.0.02,4.05,10]hexadeca-1(16),5,7,9,12,14-hexaenyl]piperazin-1-yl]-3-quinolin-5-yloxypropan-2-ol), doxorubicin (DOX; IUPAC name: (7S,9S)-7-[(2R,4S,5S,6S)-4-amino-5-hydroxy-6-methyloxan-2-yl]oxy-6,9,11-trihydroxy-9-(2-hydroxyacetyl)-4-methoxy-8,10-dihydro-7H-tetracene-5,12-dione), rifampicin (RIF; IUPAC name: [(7S,9E,11S,12R,13S,14R,15R,16R,17S,18S,19E,21Z)-2,15,17,27,29-pentahydroxy-11-methoxy-3,7,12,14,16,18,22-heptamethyl-26-[(E)-(4-methylpiperazin-1-yl)iminomethyl]-6,23-dioxo-8,30-dioxo-24-azatetracyclo[23.3.1.1^{4,7}.0^{5,28}]triaconta-1(29),2,4,9,19,21,25,27-octane-13-yl] acetate) and thioxanthone 5 (TX5; IUPAC name: 2-isopropyl-9H-thioxanthen-9-one).

1.2. Nephrotoxic agents

Renal transporters regulate the secretion/reabsorption of the most varied types of compounds playing a huge role in the development of their nephrotoxicity (Bush et al. 2017; Shen et al. 2019). Uptake transporters are frequently more efficient than efflux transporters resulting in a higher concentration of xenobiotics within the proximal tubular cell. In this way, the compounds that can cause nephrotoxicity will be in greater amounts than in normal conditions leading, indirectly, to nephrotoxicity in the form of several types of lesions (Figure 6) (Shen et al. 2019; Zhou et al. 2019). These compounds may be endogenous, like uric acid, indole derivatives, prostaglandins, bile acids, bilirubin conjugates and conjugated

steroids (Nigam et al. 2014) or exogenous (George et al. 2017). The exogenous can be divided into two major groups: therapeutic agents, which includes antibiotics [beta-lactam antibiotics (Aleksunes et al. 2008), aminoglycosides (Lopez-Novoa et al. 2011), fluoroquinolones (Ramalakshmi et al. 2003) and glycopeptide antibiotics (Elyasi et al. 2012)]; antiviral drugs (George et al. 2017); cisplatin (Silva et al. 2015b; Shen et al. 2019); cyclosporine A (Kotowski et al. 2019); non-steroidal anti-inflammatory drugs (Huerta et al. 2006; Döring and Petzinger 2014); and others xenobiotics like aristolochic acid (Nolin and Himmelfarb 2010); fluoride (Cárdenas-González et al. 2016; Quadri et al. 2018); metals [Arsenic (Orr and Bridges 2017), Cadmium (George et al. 2017) and Mercury (Genchi et al. 2017; Orr and Bridges 2017)]; Ochratoxin A (Anzai et al. 2010); Paraquat (PQ) (Chen et al. 2007; Silva et al. 2014) (Table 4). Several harmful effects on human health result from exposure to these toxic xenobiotics (Lash 2019). As already discussed, the major function of the kidney is to eliminate xenobiotics, what makes it a more susceptible organ since that the xenobiotics tend to accumulate on it.

Table 4. Transporters and nephrotoxic agents which are transported by them.

Transporter	Nephrotoxic agents	Type of lesion	References
OAT	Mercury	Tubular cell toxicity	(Genchi et al. 2017; Orr and Bridges 2017)
	Ochratoxin A	Tubular cell toxicity	(Anzai et al. 2010)
OAT1	Cephaloridine	Acute interstitial nephritis, glomerulonephritis	(Aleksunes et al. 2008)
	Acyclovir	Acute interstitial nephritis, crystal nephropathy	(George et al. 2017)
	Penicillin G	Acute interstitial nephritis, glomerulonephritis	(Aleksunes et al. 2008)
	Adefovir	Tubular cell toxicity	(George et al. 2017)
	Cidofovir	Tubular cell toxicity	(George et al. 2017)
	Tenofovir	Tubular cell toxicity	(George et al. 2017)
	Aristolochic acid	"Chinese herb nephropathy", Balkan endemic nephropathy	(Nolin and Himmelfarb 2010)
	NSAIDs	Acute interstitial nephritis, chronic interstitial nephritis, intraglomerular hemodynamics alteration	(Huerta et al. 2006; Döring and Petzinger 2014)
OAT2	Penicillin G	Acute interstitial nephritis, glomerulonephritis	(Aleksunes et al. 2008)
	Acyclovir	Acute interstitial nephritis, crystal nephropathy	(George et al. 2017)
	Aristolochic acid	"Chinese herb nephropathy", Balkan endemic nephropathy	(Nolin and Himmelfarb 2010)
OAT3	Cephaloridine	Acute interstitial nephritis, glomerulonephritis	(Aleksunes et al. 2008)
	Acyclovir	Acute interstitial nephritis, crystal nephropathy	(George et al. 2017)
	Cidofovir	Tubular cell toxicity	(George et al. 2017)
	Tenofovir	Tubular cell toxicity	(George et al. 2017)
	Aristolochic acid	"Chinese herb nephropathy", Balkan endemic nephropathy	(Nolin and Himmelfarb 2010)
OCT	Paraquat	Renal dysfunction by acute renal failure and, then, acute oliguric renal failure	(Chen et al. 2007; Silva et al. 2014)

OCT2	Gentamicin	Tubular cell toxicity	(Lopez-Novoa et al. 2011)
	Cisplatin	Tubular cell toxicity	(Silva et al. 2015b; Shen et al. 2019)
	Cadmium	Renal dysfunction by Fanconi-type syndrome, nephrolithiasis, and hypercalciuria	(George et al. 2017)
OATP1A2	Levofloxacin	Acute interstitial nephritis, crystal nephropathy	(Ramalakshmi et al. 2003)
OATP2B1	Arsenic	Fanconi syndrome, tubular cell toxicity	(Orr and Bridges 2017)
OCTN1	Cephaloridine	Acute interstitial nephritis, glomerulonephritis	(Aleksunes et al. 2008)
PEPT1	Acyclovir	Acute interstitial nephritis, crystal nephropathy	(George et al. 2017)
MRP1	Adefovir	Tubular cell toxicity	(George et al. 2017)
	Arsenic	Fanconi syndrome, tubular cell toxicity	(Orr and Bridges 2017)
MRP2	Mercury	Tubular cell toxicity	(Genchi et al. 2017; Orr and Bridges 2017)
	Arsenic	Fanconi syndrome, tubular cell toxicity	(Orr and Bridges, 2017)
MRP4	Tenofovir	Tubular cell toxicity	(George et al. 2017)
	Levofloxacin	Acute interstitial nephritis, crystal nephropathy	(Ramalakshmi et al. 2003)
P-gp	Arsenic	Fanconi syndrome, tubular cell toxicity	(Orr and Bridges 2017)
	Cyclosporine	Decreased glomerular filtration rate, hypertension	(Kotowski et al. 2019)
	Cisplatin	Tubular cell toxicity	(Silva et al. 2015b; Shen et al. 2019)
	Paraquat	Renal dysfunction by acute renal failure and, then, acute oliguric renal failure	(Chen et al. 2007; Silva et al. 2014)
	Tenofovir	Tubular cell toxicity	(George et al. 2017)
	Mercury	Tubular cell toxicity	(Genchi et al. 2017; Orr and Bridges 2017)
BCRP	Penicillin G	Acute interstitial nephritis, glomerulonephritis	(Aleksunes et al. 2008)
	Paraquat	Renal dysfunction by acute renal failure and, then, acute oliguric renal failure	(Chen et al. 2007; Silva et al. 2014)
MATE1	Cadmium	Renal dysfunction by Fanconi-type syndrome, nephrolithiasis, and hypercalciuria	(George et al. 2017)
	Cisplatin	Tubular cell toxicity	(Silva et al. 2015b; Shen et al. 2019)
	Acyclovir	Acute interstitial nephritis, crystal nephropathy	(George et al. 2017)
	Levofloxacin	Acute interstitial nephritis, crystal nephropathy	(Ramalakshmi et al. 2003)
MATE2-K	Levofloxacin	Acute interstitial nephritis, crystal nephropathy	(Ramalakshmi et al. 2003)
	Acyclovir	Acute interstitial nephritis, crystal nephropathy	(George et al. 2017)
	Cisplatin	Tubular cell toxicity	(Silva et al. 2015b; Shen et al. 2019)
	Cadmium	Renal dysfunction by Fanconi-type syndrome, nephrolithiasis, and hypercalciuria	(George et al. 2017)

Legend: NSAID. Non-steroid anti-inflammatory drug.

As previously mentioned, knowing the different drug interactions associated with P-gp, it will be possible to modulate the activity of this transporter aiming to reduce the drug-induced nephrotoxicity (induction/activation) or, alternatively, to increase the therapeutic effect of drugs, especially those targeted to the kidney. One example of this modulation is the

interaction that happens on P-gp transport between digoxin, which is a probe drug for P-gp, and quinidine or ritonavir, which are P-gp inhibitors. Their coadministration results in an increase of digoxin plasma levels and a decrease of the digoxin renal clearance, suggesting that the P-gp-mediated transport of digoxin may be inhibited at the kidney level (Akamine et al. 2012; Yin and Wang 2016).

In this study, we study the possibility of modulating P-gp transport activity using the compounds already discussed and cisplatin as a known nephrotoxic agent. In that way, cisplatin will be described with more detail in the following section.

1.2.1. Cisplatin

Cisplatin (cis-diamminedichloroplatinum II; Platinol; CP; Figure 8) was the first platinum-based antineoplastic to be discovered and it is one of the most effective chemotherapeutic agents currently used in the treatment of several malignant diseases, including head and neck, esophageal, bladder, testicular, ovarian, uterine, cervical, breast, stomach, non-small and small-cell lung cancers (Harrach and Ciarimboli 2015; Crona et al. 2017; Volarevic et al. 2019).

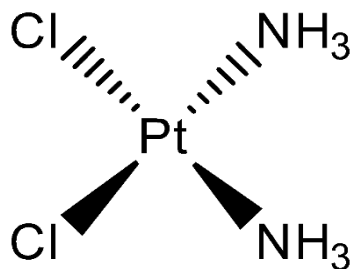


Figure 8. Cisplatin chemical structure.

Its mechanisms of action on the tumoral cells are:

- DNA damage: this drug binds to adjacent purine bases altering the secondary structure of DNA, which inhibits its function template and DNA replication;
- cytoplasmic organelle dysfunction: with endoplasmic reticulum stress and mitochondrial dysfunction;
- affectation of tumor-suppressor protein p53;
- apoptotic pathways both caspase-dependent and receptor-mediated death;
- oxidative stress: with formation of reactive oxygen species and depletion of GSH, an antioxidant;
- inflammation: mediated via tumor necrosis factor and other chemokines.

All these pathways will lead to induction of apoptosis of the tumoral cells (Arany and Safirstein 2003; Manohar and Leung 2017). However, cisplatin treatment has some serious side effects, such as nephrotoxicity, more specifically in the kidney proximal tubule epithelial cells; neurotoxicity, in the upper and lower extremities; and ototoxicity, within the mechanosensory outer hair cells of the cochlea (Karasawa and Steyger 2015). Its mechanisms of action, brilliantly used as antineoplastic agents, have consequences in other cells that are not the target tumour cells. CP nephrotoxicity is a serious renal complication in patients receiving CP-based chemotherapy seen in 30 to 40% of patients. It is known to cause tubular damage, inflammatory damage to the interstitium and vascular injury, as well as acute kidney injury (AKI) which, eventually, leads to chronic kidney disease (CKD) (Manohar and Leung 2017; Shi et al. 2018; Volarevic et al. 2019). Thus, this will be a limiting factor in the dose and/or intensity of the dose used in these patients (Crona et al. 2017). Currently, the relief or prevention of nephrotoxicity caused by CP is carried out by hydration, magnesium supplementation or by forced diuresis induced by mannitol. However, treatment with mannitol causes super diuresis and consequent dehydration, demanding an urgent need for the clinical application of a safe and effective kidney protective drug, as an additive therapy for patients treated with CP in high doses (Volarevic et al. 2019). The biggest challenge is to find a drug that reduces the side effects of cisplatin without decreasing its antineoplastic potential (Manohar and Leung 2017).

In the kidney, the influx of cisplatin is performed by OCT2 and copper transporter 1 (CTR1; SLC31A1), basolateral transporters of proximal tubular cells (see **1.1. Renal Transporters**). OCT2 is a transporter whose activity depends on the ATP or transmembrane ion flux. In that way, the plasma membrane potential creates both an electrical and a concentration gradient for its cationic substrates. This allows an accumulation of platinum derivatives into the cells to intracellular concentrations exceeding the extracellular level. Thus, down-regulation of these transporters has been studied in order to decrease the entry of cisplatin into the renal cells and, consequently, their intracellular concentration (Harrach and Ciarimboli 2015). The efflux is performed by MATE1, MRP2 and P-gp, apical transporters (Silva et al. 2015b; Shen et al. 2019). The combined activity of these transporters determines the inexistence of cisplatin accumulation, which will correlate with nephrotoxicity (Vormann et al. 2018). Thus, it is important to study the cisplatin efflux transporters from renal tubular cells aiming to regulate their activity in order to increase the export of this nephrotoxic, decreasing its intracellular concentration and the respective nephrotoxicity. In the present study, we analyze the P-gp *in vitro* induction/activation on HK2 cells and the decrease of cisplatin-induced nephrotoxicity due to this P-gp modulation.

1.3. Aims

The general objective of this work is to prove that it is possible to reduce the toxicity of P-gp toxic substrates, modeling its expression and/or activity in renal tubular cells (HK2).

There are some specific objectives that must be fulfilled:

- verify P-gp expression levels on HK2 cells;
- access the cytotoxicity profile of the compounds used as inhibitor (ZOS), inducers/activators (TX5, DOX, RIF) and even substrates (RHO 123) in HK2 cells;
- evaluate compounds's-mediated modulation of P-gp activity and/or expression;
- verify the potential protection against cisplatin (toxic P-gp substrate) cytotoxicity by P-gp inducers and activators in HK2 cells.

2. MATERIAL AND METHODS

2.1. Materials

Reagents used in cell culture, including RPMI medium (1640, #21875-034), fetal bovine serum (FBS) (#10270-106), Penicillin-Streptomycin (#15140-122), 0.05% trypsin/1 mM EDTA (#25300-054), and Hanks' Balanced Salt solution (+/+) (HBSS, [+] Calcium chloride, [+] Magnesium chloride; #14025-092) were purchased from Gibco. Phosphate-buffered saline solution (PBS) was made by TRECARD (Translational Research on Renal and Cardiovascular Diseases) department of the University of Salamanca, containing 139 mM NaCl, 2.6 mM KH_2PO_4 , 4.1 mM Na_2HPO_4 . L-Glutamine (#SLBF97892), also used in cell culture, as well as zosuquidar (#SML1044), doxorubicin (#44583), rhodamine 123 (2-(6-Amino-3-imino-3H-xanthen-9-yl) benzoic acid methyl ester, RHO 123, #R8004), 3-(4,5-dimethylthiazol-2-yl)-2,5-diphenyl tetrazolium bromide (MTT, #MKCF0652) and cisplatin (cis-diamminedichloroplatinum II, CP, #P4394) were obtained from Sigma (St. Louis, MO, USA). Western Blotting reagents were purchased from Bio-Rad Laboratories (Hercules, California, USA). All the reagents used were of analytical grade or of the highest grade available. 1-(propan-2-ylamino)-4-propoxy-9H-thioxanthen-9-one (TX5) was synthesized by the Organic and Pharmaceutical Chemistry Laboratory of the Faculty of Pharmacy of University of Porto, according to described procedures.

2.2. HK2 cells culture

All cell culture procedures were performed in a laminar flow chamber using sterile material. HK2 cells were routinely cultured in 100 mm plates (58.1 cm²) and incubated at 37 °C in a humid atmosphere, with 5% CO₂ – 95% air atmosphere. The preparation of the culture medium was made using RPMI medium and adding 10% FBS (without inactivation); 1 mM L-Glutamine; and 500 U/mL Penicillin-Streptomycin.

To maintain the cell culture, the cultures were passed by trypsinization when the cells had grown attached to the plate and were confluent. To pass the cells, the medium was first removed by aspirating with a vacuum pump and two washes with 5 mL PBS were performed to remove the remains of the medium. Then, 2 mL of trypsin was added and was left to act for one minute (37 °C, 5% CO₂ – 95% air atmosphere), in order to detach and lift the cells from the plate. Subsequently, 6mL of cell culture medium were added (at least three times the amount of trypsin) to inactivate the trypsin, the cells suspension transferred to centrifuge tube and the content was centrifuged for 3 min at 600 xg, in order to eliminate the remains

of trypsin that remained in the supernatant along with the medium. After decanting the cell culture medium, a pellet corresponding to the cells was obtained, which was resuspended in 1 mL of cell culture medium and then 8 mL were added to seed them into the new plates. The final volume in each plate was 8 - 9 mL. Passes 1:4 - 1:5 were performed every 3 - 4 days and the medium was renewed 2 - 3 days a week until the cells reached confluence again.

In order to perform the experiments, after trypsinizing, centrifuging, resuspending, and counting, the HK2 cells were seeded in 24-well plates (2 cm²) and used 1 day after seeding. To count the cells, an homogeneous mixture of 10 µl of the cell suspension and 10 µl of 0.4% Trypan Blue in PBS (1:1) was prepared and added to the edge of the Neubauer chamber coverslip, allowing dispersion of the mixture by capillary action between the grids. Neubauer's camera is a slide that consists of two parts. In each one, there is a grid at the bottom divided into 9 big squares (Figure 9) with an area of 1 mm² each and, when placing a coverslip on the camera, it leaves, in each grid, a space of 0.1 mm in height, so the total volume in each cell is 0.1 µL. HK2 cells were observed under the light microscope and the number of viable cells (that distinguish themselves from dead cells presented in blue) in 10 squares, those in the corners and the center on both sides of the chamber, was counted (Figure 9).

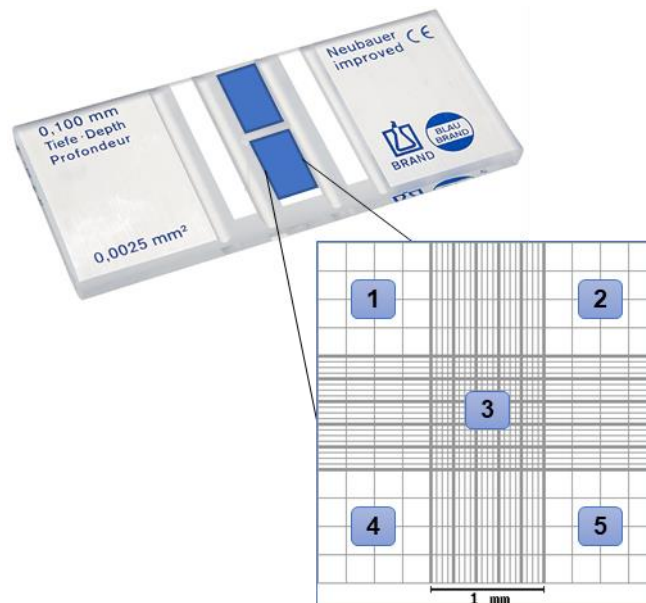


Figure 9. Neubauer chamber. Numbers 1 - 5 represents the cells used to count HK2 cells.

To obtain the volume necessary to add to each plate or plate well was used the formula described in the Figure 10.

$\text{Number of cells / } \mu\text{L} = \frac{\text{Number of cells counted} \times \text{Dilution}}{\text{Cells counted (mm}^2\text{)} \times \text{Chamber depth (mm)}}$

Figure 10. Formula used to determine the number of cells in one microliter and, consequently, the volume to add to each well to obtain a given cell density and perform the following experiments.

2.3. P-glycoprotein expression in HK2 cells

To carry out the experiments, the Western Blotting technique was performed. To that, HK2 cells were seeded in 60 mm plates (4 plates, 21.3 cm²), at a density of 17500 cells/cm² and a final volume in each well of 2000 μ L. Twenty-four hours after seeding the cells, the cell culture medium of two plates was removed, the cells washed 2 times with PBS, and a new cell culture medium without FBS was added. This change of cell culture medium is carried out to stop cell growth. The cellular lysis was carried out 24 h later. The plates were placed on ice and washed two times with 1 mL PBS each. Then, the cellular proteins were extracted with 100 μ L of lysis buffer [140 mM NaCl; 10 mM EDTA; 10% glycerol; 1% NP-40; 20 mM Tris 1 M pH 7.5, supplemented with phosphate/protease inhibitors (10 μ g/mL leupeptin; 2 μ g/mL aprotinin; 1 mM PMSF; 10 mM NaF and 1 mM Na₃VO₄)]. The plates were then scratched, and the content was picked and centrifuged (4 °C, 10 min, 10000 mg). Samples (the supernatant) were stored at -20 °C until analysis. Using Bio-Rad DC protein assay (Bio-Rad Laboratories, Hercules, CA, USA) and BSA as standard, the samples protein content was quantified.

Samples were diluted to equal protein concentration and forty micrograms of protein were loaded and separated in a 15% SDS/polyacrylamide gel, at a constant voltage of 130 mV, using a running buffer [10% Tris Glycine 10x (#161-0771, Biorad); 5% SDS (20%, #161-0418, Bio-Rad Laboratories); 85% H₂O]. 15% Running gel [23% H₂O; 50% acrylamide mix (30%); 25% Tris (1.5 M, pH 8.8); 1% ammonium persulfate (10%); 0.04% TEMED] was prepared, manually. 5% Stacking gel [60% H₂O; 17% acrylamide mix (30%); 12.5% Tris (1.5 M, pH 8.8); 1% ammonium persulfate (10%); 0.1% TEMED] was also made manually. After electrophoresis, gel was allowed to equilibrate in transfer buffer [20% Trans Blot turbo 5x Transfer Buffer (Biorad); 20% methanol; 60% H₂O] and then transferred to PVDF membranes (Trans blot turbo Midi size PVDF membrane), at a constant amperage of 2.5 A, for 7 min, in a TransBlot® Turbo™ Transfer System (Bio-Rad Laboratories). Membrane

was rinsed in washing buffer [0.2% Tris (1 M, pH 7.5); 0.5% NaCl (3M); 0.97% H₂O; supplemented with 1 mL de Tween 20 (0.1%)] and, then, its nonspecific sites were blocked for 1 h, at room temperature, in blocking buffer [3% BSA in washing buffer]. Membranes were incubated with primary antibody (overnight at 4 °C): C219 mouse monoclonal anti-P-gp (1:500, Calbiochem®, Merck KGaA, Darmstadt, Germany). After washing three times (7 min each), the membrane was then incubated with the anti-mouse IgG-peroxidase secondary antibody (1:10000; #6300-05, Southern Biotech, Birmingham, Alabama, USA), for 45 min, at room temperature. All antibodies were diluted in the blocking buffer. After carrying out three washes (7 min each, with a washing buffer), the detection took place. The immunoreactive bands and digital images were acquired using a ChemiDoc™ MP Imaging System (Bio-Rad Laboratories).

2.4. Cytotoxicity essays

In order to establish the highest non-cytotoxic concentration of each compound used in this study, cytotoxicity experiments were performed on the HK2 cell line by MTT assays. Different concentrations of zosuquidar (ZOS), thioxanthone 5 (TX5), rifampicin (RIF), doxorubicin (DOX) and rhodamine 123 (RHO 123) were tested in HK2 cells. To carry out the experiments, the cells were seeded in 24-well plates (2.00 cm²), with a density of 17500 cells/cm², in a final volume in each well of 500 µL, and used 24 h after seeding. The cell treatment time with these compounds was 24 h for ZOS, TX5, RIF and DOX. Regarding RHO 123, the exposure time was 2 h. Figure 11 shows the experimental design used in the different treatments, including the concentrations of each compound used. Furthermore, ZOS, TX5, DOX and RIF were dissolved in DMSO, a compound potentially toxic to cells (Galvao et al. 2014), its cytotoxicity was also studied, using its maximum concentration in which the compound was dissolved. RHO 123 was dissolved in PBS, which does not represent any problem to HK2 cells. Also, in each experiment, a plate of cells was seeded to carry out the MTT test at time zero (plate at time 0 h) and, thus, the cell viability before treatment was known.

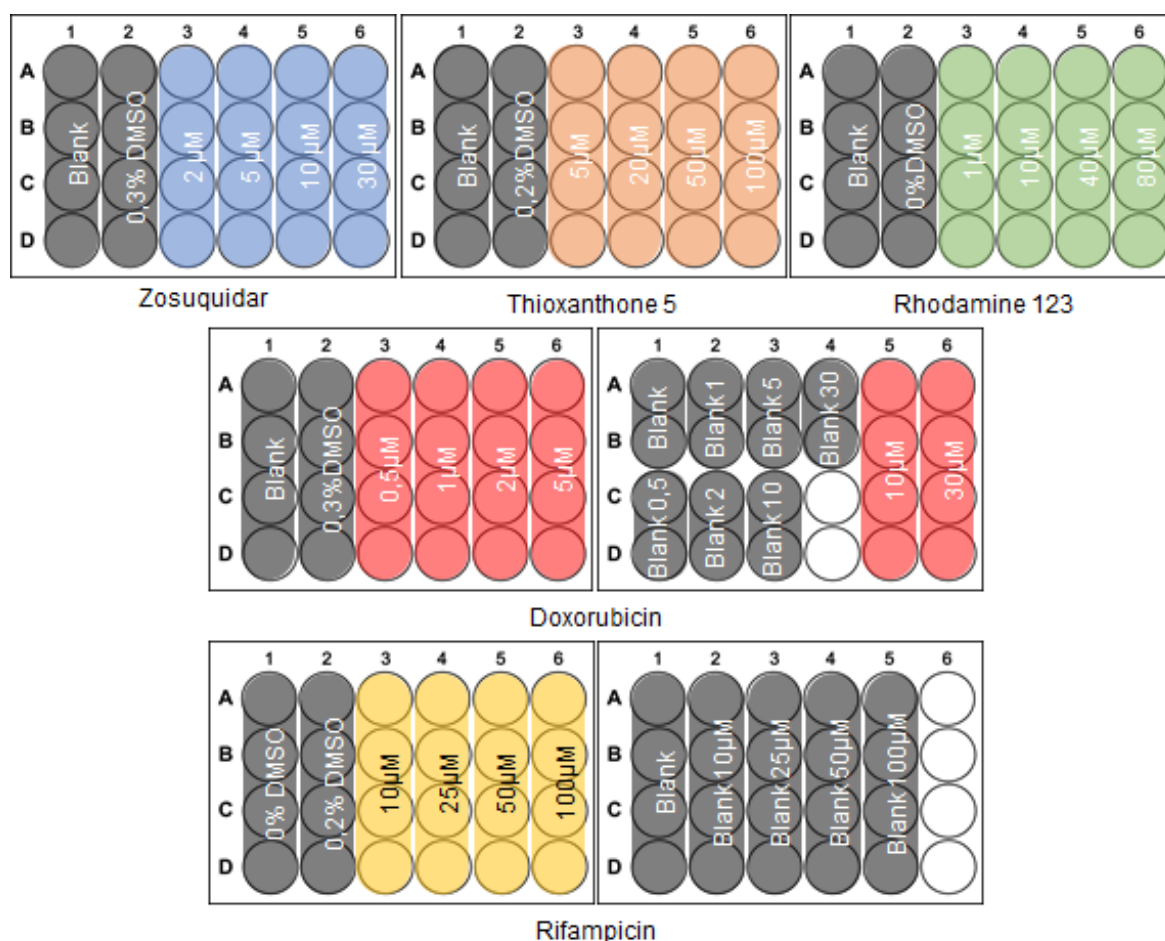


Figure 11. Experimental design of zosuquidar (ZOS), thioxanthone 5 (TX5), rhodamine 123 (RHO 123), doxorubicin (DOX) and rifampicin (RIF) cytotoxicity experiments, by incubation for 2 h/24 h in HK2 cells.

After the exposure times, the MTT assay was performed to determine cell cytotoxicity after treatment with the compounds. MTT is a yellow tetrazolium salt in aqueous solution. In living cells, MTT is reduced by mitochondrial dehydrogenases, forming formazan crystals, a blue-purple precipitate. The absorbance of this solution at 595 nm is directly proportional to the number of metabolically active (viable) cells in culture (Kumar et al. 2018). The performed procedure consisted of adding to each well, without removing the cell culture medium, 50 μ L of MTT and left to incubate 4 h at 37°C in a humidified, 5% CO₂ – 95% air atmosphere (MTT final concentration in the well of 0.05 mg/mL). During this time, formazan crystals were formed. Then, 500 μ L of 10% SDS in 0.01 M HCl was added to dissolve the produced formazan crystals and kept overnight at 37°C in a humidified, 5% CO₂ – 95% air atmosphere, in the dark. The next day, the absorbance at 595nm was measured in a multi-well plate reader (ELx800, BioTek Instruments, Vermont, USA). The percentage of MTT reduction relative to the control cells including DMSO was used as the cytotoxicity measure.

2.5. Evaluation of P-glycoprotein transport activity

The P-gp transport activity was evaluated, using rhodamine 123 (RHO 123) as a P-gp fluorescent substrate, in two different protocols: RHO 123 efflux in cells pre-exposed for 30 min, which evaluates the potential compounds-mediated P-gp activation, and RHO 123 efflux in cells pre-exposed for 24, 48 and 72 h, which evaluates potential effects on P-gp activity as a result of P-gp induction. To carry out the experiments, the cells were seeded in 24-well plates (2 cm²), at a density of 50000 cells/cm², in a final volume in each well of 500 µL and used 24 h after seeding.

2.5.1. RHO 123 efflux assay in cells pre-exposed for 30 minutes

The culture medium from all wells of the 24-well plate was aspirated. HK2 cells were exposed to TX5 (20 µM), DOX (2 µM) and RIF (20 µM), in HBSS, as schematized in the Figure 12, for 30 min, at 37°C in a humidified atmosphere of 5% CO₂ - 95% air atmosphere. The concentration of 1 µM ZOS, the specific P-gp inhibitor, was previously optimized for the present experimental conditions.

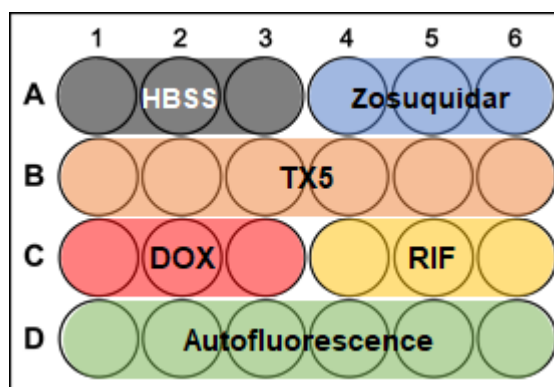


Figure 12. Experimental design of the rhodamine 123 (RHO 123) efflux assays, with a 30-minutes exposure in HK2 cells to zosuquidar (ZOS; 1 µM), thioxanthone 5 (TX5; 20 µM), doxorubicin (DOX; 2 µM) and rifampicin (RIF; 20 µM).

After the pre-incubation period, 50 µL of RHO 123 (final concentration of 10 µM) was added to the first 3 lines (Figure 12 - Lines A, B and C) and incubated for 90 min (37 °C, 5% CO₂ - 95% air atmosphere). Then, the medium containing RHO 123 was aspirated and the cells washed 2 times with Hanks' Balanced Salt solution (HBSS) +/+. The following step was the addition of 250 µL of 0.1% Triton x100 (#T8787, Sigma, St. Louis, MO, USA) and incubation,

for 30 min at room temperature, to occur the cell lysis and the release of the intracellular RHO 123 content. The fluorescence was read in the Fluoroskan Ascent FL (Thermo Electron Corporation, Waltham, Massachusetts, USA) at excitation and emission wavelengths of 485/20 and 528/20 nm, respectively, and expressed as fluorescence intensity (FI). The autofluorescence was removed at these values and their inverse (1/FI) was calculated, which indicates the P-gp activity. Results were expressed as a percentage of P-gp activity compared to control cells (100%).

2.5.2. RHO 123 efflux assay with pre-exposition for 24, 48 and 72 hours

The culture medium was aspirated from all wells of the 24-well plate. The solutions of TX5 (20 μ M), DOX (2 μ M), RIF (20 μ M) were added to the respective well, as schematized in the Figure 14, for 24, 48 and 72 min, at 37 °C in a humidified atmosphere of 5% CO₂ - 95% air atmosphere. After the pre-incubation period, 50 μ L of RHO 123 (10 μ M final concentration) was added to the first 2 lines (Figure 13 - Lines A and B) and the plates were incubated for 90 min (37 °C, 5 % CO₂ - 95% air atmosphere). After this incubation period, the medium containing RHO 123 was aspirated and the cells washed 2 times with HBSS (+/+). Thereafter, 250 μ L of 0.1% Triton x100 were added to the plates and an incubation of 30 min at room temperature was performed. The fluorescence was then read in the Fluoroskan Ascent FL (Thermo Electron Corporation, Waltham, Massachusetts, USA) at excitation and emission wavelengths of 485/20 and 528/20 nm, respectively, and expressed as FI. The autofluorescence was removed at these values and their inverse (1/FI) was calculated, which indicates the P-gp activity. Results were expressed as a percentage of P-gp activity compared to control cells (100%).

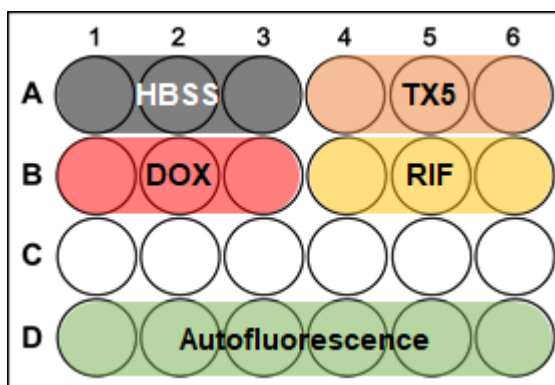


Figure 13. Experimental design of the rhodamine 123 (RHO 123) efflux assays, with a 24, 48 and 72-hours HK2 cells exposure to thioxanthone 5 (TX5; 20 μ M), doxorubicin (DOX; 2 μ M) and rifampicin (RIF; 20 μ M).

2.6. Cisplatin-induced cytotoxicity assays

To perform these experiments, the HK2 cells were seeded in 24-well plates (2.00 cm²), at a density of 17500 cells/cm² and in a final volume in each well of 500 µL. Twenty-four hours after seeding, plates were washed two times with PBS to eliminate the FBS, and HK2 were exposed to the compounds (2 µM DOX; 20 µM RIF; 20 µM TX5 or 1 µM ZOS, prepared in cell culture medium without FBS). The exposure was carried in three different conditions:

- Exposure to DOX, RIF, TX5 or ZOS for 30 min, with posterior aspiration of these solutions and two washes with PBS (before the exposure to cisplatin for 18 h), simulating the conditions performed in the activation assays.
- Exposure to DOX, RIF or TX5 for 48 h, without removal of the compounds and washes (before the exposure to cisplatin for 18 h), simulating the conditions performed in the induction assays.
- Exposure to DOX, RIF or TX5 for 30 h, without removal of the compounds and washes (before the exposure to cisplatin for 18 h), completing an exposure time of 48h, simulating the conditions performed in the induction assays.

After this treatment time, HK2 were exposed to CP (10 µM, 30 µM and 300 µM, prepared in cell culture medium without FBS) for 18 h. The selected cisplatin concentrations were previously optimized, knowing that with a concentration of 10 µM CP has an anti-proliferative effect, with a concentration of 30 µM CP has an apoptotic and with a concentration of 300 µM CP has a necrotic effect (Sancho-Martínez et al. 2011, 2018). The experimental design of each plate is represented in Figure 14.

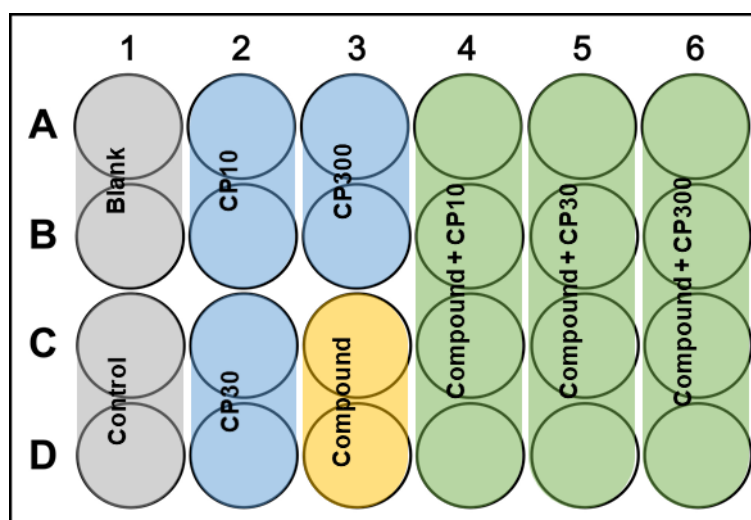


Figure 14. Experimental design of the cisplatin cytotoxicity assays. Legend: CP. Cisplatin. Compound: doxorubicin (2 µM), rifampicin (20 µM), thioxanthone 5 (20 µM) or zosuquidar (1 µM).

Before the MTT assay, photos were made using the optic microscope and the Software AxioVision (Carl Zeiss Microscopy GmbH, Oberkochen, Germany). The MTT assays were carried out under the same experimental conditions described in section **2.4. Cytotoxicity assays**.

2.7. Statistical analysis

All data is expressed as mean \pm standard error of the mean of three experiments with triplicates/quadruplicates. Statistical analysis was performed with IBM SPSS Statistics® 26. The normality test was initially carried by Kolmogorov-Smirnov, which indicated that our data contained normal values. Then the Kruskal-Wallis Test was used to statistically analyze all the data. Significant differences with p-value below 0.05 were considered.

3. RESULTS AND DISCUSSION

3.1. P-glycoprotein expression on HK2 cells

As previously described, this study started by confirming that P-gp is present in the studied cells, the HK2 cells. This confirmation was carried out by Western Blotting, which separates proteins according to their molecular weight. The molecular weight of P-gp is 170 kDa (Martins et al. 2019). The use of the primary antibody C219 mouse monoclonal anti-P-gp resulted not only in the appearance of a band in the 170 kDa, corresponding to P-gp, but also to a set of other non-specific bands (Figure 15).

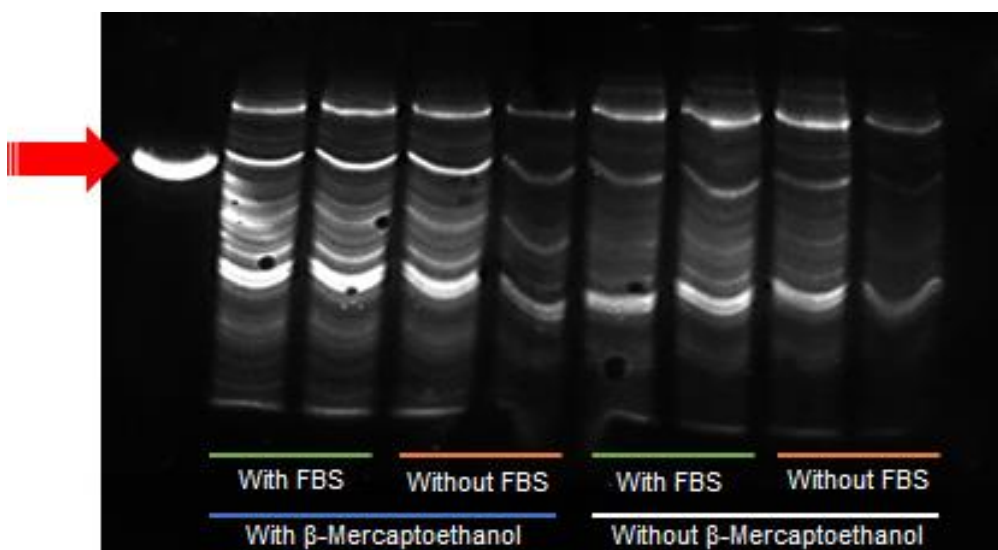


Figure 15. Chemiluminescent image obtained in the membrane incubated with the primary antibody C219 mouse monoclonal anti-P-gp and the anti-mouse IgG-peroxidase secondary antibody. Red arrow represents the molecular weight of 170 kDa. Samples represented with green were obtained in the protein extraction from HK2 cells in culture medium with fetal bovine serum (FBS). Samples represented with orange were obtained in the protein extraction from HK2 cells in culture medium without FBS. To the samples represented in blue was added β -Mercaptoethanol.

With this protein separation technique it was possible to observe a band corresponding to the molecular weight of P-gp (Figure 15), leading us to conclude that this efflux protein is actually present in the HK2 cells used in the present study. Furthermore, observing the experimental conditions tested, it was possible to note that HK2 cells maintained in culture medium with FBS present a higher expression of P-gp. In this way, culture medium with FBS was used in the following assays. On the other hand, samples, to which β -mercaptoethanol was added at sample preparation, presented a better definition of the bands.

In accordance, some articles have also shown the presence of P-gp on HK2 cells. Tramonti et al identified P-gp presence in this immortalized cell line, using Western blotting, showing for the first time the presence of a functional P-gp on HK2 cells (Tramonti et al. 2001). Later, Romiti et al also showed a well-defined band at approximately 150 kDa in the Western blots of crude membranes of HK2 cells (Romiti et al. 2002). On the other hand, Jenkinson et al investigated the expression and function of some drug transporters in HK2 cells and their suitability as an *in vitro* model of the human proximal tubule, observing the presence of P-gp (Jenkinson et al. 2012).

In general, the HK2 cell line has been described as an adequate tool for *in vitro* studies on P-gp-dependent human renal transport mechanisms (Tramonti et al. 2001). This makes it a good choice for the present study, since, also here, the existence of P-gp in these cells was confirmed.

3.2. Cytotoxicity assays

After the observation of the presence of P-gp on HK2 cells, the safety/cytotoxicity tests of ZOS, TX5, RIF, DOX and RHO 123 were carried out. Figure 16 presents the compounds cytotoxicity (in percentage of control + DMSO) obtained for each concentration of all studied compounds, which were statistically compared to control and to control with DMSO. DMSO cytotoxicity was also controlled since it is a compound potentially toxic to cells (Galvao et al. 2014), in which the majority of the compounds (ZOS, TX5, RIF and DOX) were dissolved, as described in **2.4. Cytotoxicity assays**. However, in our study, DMSO did not cause any significant variation in these cells growth. With ZOS, used as a known inhibitor of P-gp (Mollazadeh et al. 2018), concentrations of 2, 5, 10 and 30 μ M were tested. Previous studies in this area, not only in HK2 cells but also in other cell lines, aided the selection of the concentrations of ZOS (Nies et al. 2008; Arakawa et al. 2019), TX5 (Silva et al. 2014, 2015a), RIF (Harmsen et al. 2010; Vilas-Boas et al. 2013b), DOX (Park et al. 2012; Silva et al. 2013) and RHO 123 (Chieli et al. 2012; Lopes et al. 2018) to be studied in this phase.

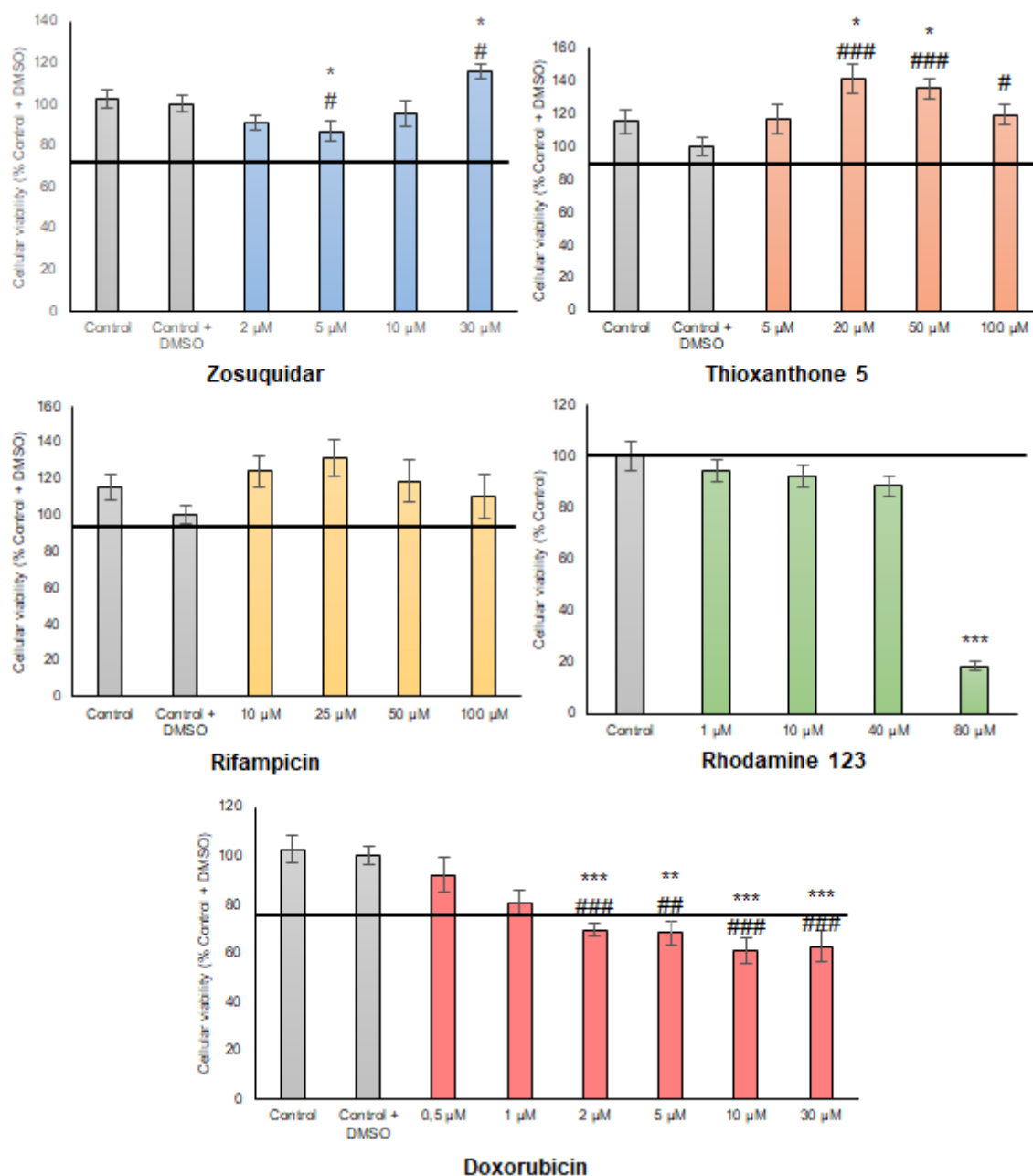


Figure 16. Cell viability (% Control + DMSO) of HK2 cells exposed to different concentrations of zosuquidar, thioxanthone 5, rifampicin and doxorubicin, for 24 h, and rhodamine 123, for 2 h, based on the MTT assays. Data is presented as mean \pm standard error of 3 experiments with quadruplicates (n=12). Black line represents cell viability before treatment (time 0). *: p<0.05, **: p<0.01 and ***: p<0.001, compared with Control; #: p<0.05, ##: p<0.01 and ###: p<0.001, compared with Control + DMSO.

Despite some statistically significant cell viability decrease (5 μ M ZOS, compared to control or control + DMSO) shown in the graph, all the concentrations were higher than the time 0 line, showing that none of the concentrations used is considered cytotoxic at 24 h of incubation (although there may be an antiproliferative effect). On the other side, in HK2 cells exposed to 30 μ M ZOS, it was possible to observe a proliferative effect. Relatively to the inducers/activators used in the present study, TX5 was tested at concentrations 5, 20,

50 and 100 μM ; RIF was tested at concentrations of 10, 25, 50 and 100 μM ; and DOX was tested at concentrations of 0.5, 1, 2, 5, 10 and 30 μM . The obtained results were very similar, showing that these concentrations were non-cytotoxic to HK2 cells at 24h of incubation, since there were no significant differences between their tested concentrations and the time 0 line; however, it is possible to see an antiproliferative effect in HK2 cells exposed to DOX at concentrations of 2, 5, 10 and 30 μM . Regarding the known substrate of P-gp, RHO 123, the concentrations of 1, 10, 40 and 80 μM were tested. In this graph, it is possible to observe a statistically significant difference between the concentration of 80 μM and the control and the other concentrations tested, having been classified as a cytotoxic concentration of RHO 123 for HK2 cells.

Therefore, after analyzing these results, the concentration of each compound to be used in the next tests was chosen, taking into account not only our data (presence or absence of cytotoxicity) but also previous studies that, like in the present study, used RHO 123 efflux to evaluate P-gp activity (Tramonti et al. 2001; Vilas-Boas et al. 2013b; Silva et al. 2014, 2015a, 2020; Chen et al. 2016; Lopes et al. 2018; Martins et al. 2019). The selected concentrations were 5 μM ZOS, 20 μM TX5 and 20 μM RIF, 2 μM DOX and 10 μM RHO 123.

Relatively to ZOS and TX5, no studies using HK2 cells were found in the literature. On the other hand, DOX has been extensively studied, including in HK2 cells, although several studies have demonstrated its nephrotoxicity. Park et al proved that, in HK2 cells, DOX (1, 2, 4, or 8 μM , for 24 h) decreased cell viability in a concentration-dependent manner, suggesting also that DOX induced cytotoxicity through an extracellular-signal-regulated kinase (ERK)-dependent pathway (Park et al. 2012). Su et al considered this compound as a nephrotoxic, also studying compounds that protect against renal toxicity in DOX-treated cancer patients, using HK2 cells and a mice model. This group also suggested that the nephrotoxicity caused by DOX (dose of 5 mg/kg, intraperitoneal, twice/week for 2 weeks) in these cells could be mediated by the suppression of the activation of cleaved caspase-3 and ERK1/2 pathways, factor nuclear kappa B (NF- κB) p65 and NO production (Su et al. 2015). Furthermore, a more recent study also demonstrated the nephrotoxicity induced by DOX (5 mg/kg dissolved in 0.9% normal saline, intraperitoneal, every other day for 2 weeks), using several models (*in vivo*, in Balb/c male mice, and *in vitro*, using the HK2 cell line and a normal rat kidney epithelial cell line (NRK-52E) (Zhang et al. 2020). Despite this, our results only classify DOX as anti-proliferative in the studied concentrations, using it in the following experiments as a potential inducer/activator. There are also some studies in which HK2 cells are exposed to RIF. Knowing its role in inducing P-gp, Chen et al exposed

this cell line, as well as other like the HepG2 and Madin-Darby canine kidney (MDCK) cell lines, to RIF in order to increase the efflux of quantum dots (QDs), reducing their hepatic and renal toxicity. This group of researchers tested concentrations of 10, 25 and 50 μM (24 h), which proved to be non-cytotoxic in all studied cell lines (including HK2 cells) (Chen et al. 2016). Another example is a study reported by Wang et al, who performed treatments with RIF 10 μM in HK2 cells for 48 h, without observing any cytotoxicity (Wang et al. 2013).

3.3. Evaluation of P-glycoprotein transport activity

P-gp modulation, particularly inhibition, induction, and activation, was evaluated using RHO 123 accumulation assays in two different experimental conditions: exposure to inductors/activators for 30 min, mimetizing activation conditions; and exposure to inductors/activators for 24, 48 or 72 h, simulating induction conditions. All the graphs represented in this section represent the inverse of the FI obtained (representing intracellular accumulation of RHO 123), thus demonstrating the activity of P-gp. Initially, a concentration of 5 μM of ZOS was used. However, this concentration was further optimized, ensuring maximal P-gp inhibition (Figure 17).

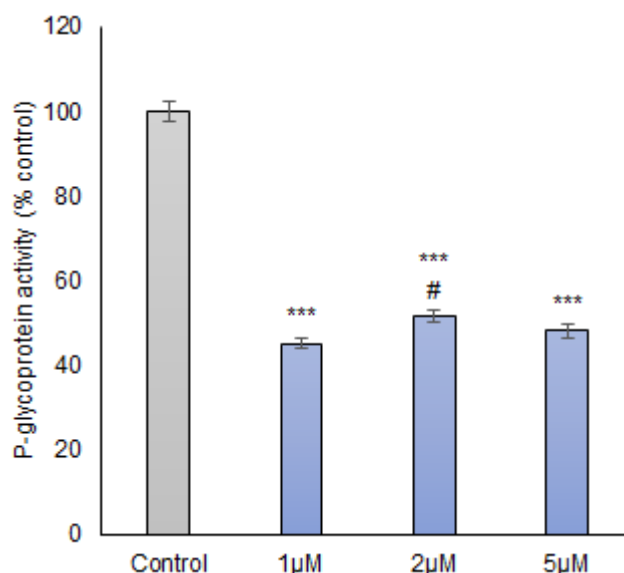


Figure 17. P-gp activity evaluated by fluorescence spectroscopy in HK2 cells through the rhodamine 123 accumulation assay performed in the presence of different ZOS concentrations (1, 2 and 5 μM , for 30 min). Grey color represents control cells. Blue color represents the results obtained for ZOS-treated cells. Data is presented as mean \pm standard error of 3 experiments with triplicates ($n=9$). ***: $p<0,001$, compared with control. #: $p<0.05$, compared with 1 μM ZOS.

Thereby, 1 μM ZOS was selected as the P-gp inhibitor concentration to be used in the following assays as positive control, since it appears to be the minimal concentration that shows the greatest decrease in P-gp activity in HK2 cells.

The results obtained for the 30-minute exposure to the tested compounds are shown in Figure 18. It is possible to observe a tendency for an increased P-gp activity in the presence of all compounds tested as inducers/activators, proving in fact their role in activating this pump. Furthermore, in the case of TX5, the increase in P-gp transport activity was significantly relevant, increasing to 111.60%, when compared to control cells (100%).

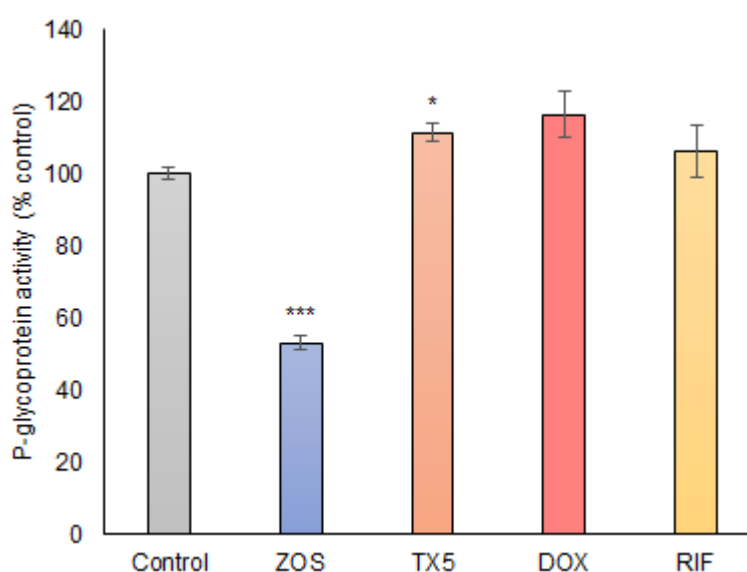


Figure 18. P-glycoprotein activity transport (% control) in HK2 cells exposed to thioxanthone 5 (TX5; 20 μM ; orange), doxorubicin (DOX; 2 μM ; red) and rifampicin (RIF; 20 μM ; yellow), for 30 min, based on rhodamine 123 assays. Grey color represents Control. Data is presented as mean \pm standard error of 3 experiments with triplicates (n=9). *: $p < 0.05$ and ***: $p < 0.001$, compared with control.

Considering the RHO 123 assay done with long time exposure, the results obtained are shown in Figure 19. In these graphs, it is possible to observe a significant increase in P-gp activity in the presence of all the compounds studied compared to the control, proving their P-gp induction. Furthermore, after performing the statistical analysis, no significant differences were observed between the exposure times, demonstrating that exposure times of 24, 48 or 72h causes similar P-gp induction. Therefore, the exposure time of 48 h was chosen to carry out the next experiments.

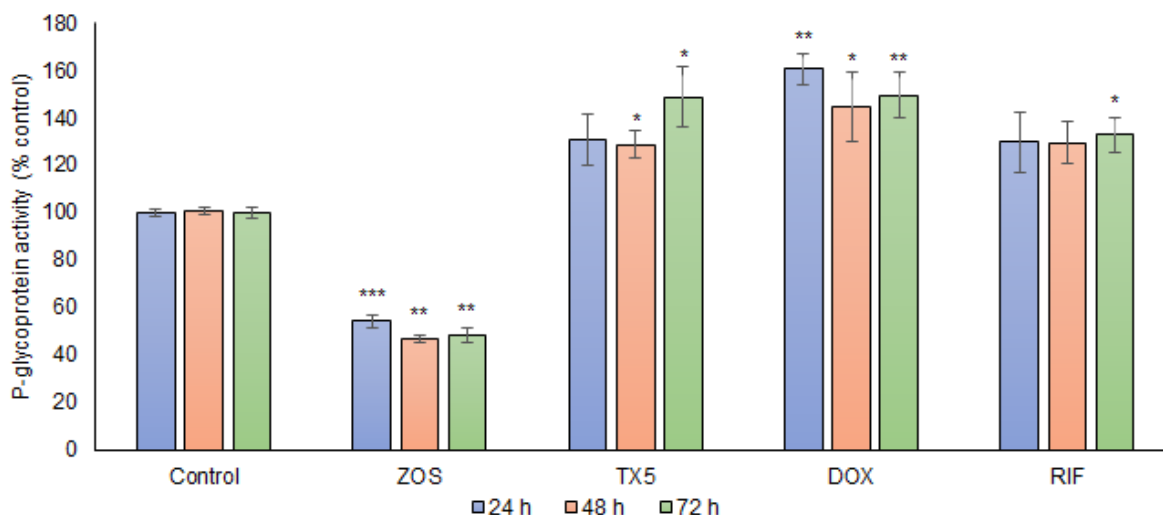


Figure 19. P-glycoprotein activity transport (% control) in HK2 cells exposed to thioxanthone 5 (TX5; 20 μ M), doxorubicin (DOX; 2 μ M) and rifampicin (RIF; 20 μ M), for 24 (blue), 48 (orange) and 72 h (green), based on RHO 123 assays. Data is presented as mean \pm standard error of 3 experiments with triplicates (n=9). *: p<0.05, **: p<0.01 and ***: p<0.001, compared with control.

RHO 123 is a membrane-permeable fluorescent dye that is widely used to evaluate the P-gp functional transport activity, since it is a rapid and simple method that can be used in drug transport studies in different *in vitro* models (Iqbal et al. 2005). Some studies are described in the literature in which RHO 123 to determine the activity of this pump in HK2 cells. Tramonti et al was the first to perform this type of analysis on HK2 cells, incubating them with RHO 123 (5 μ g/mL) for 60 min, exposing them to possible inhibitors (by washing the cells with medium containing them) and, then, extracting the intracellular dye with n-butanol. They showed that verapamil and cyclosporin A significantly inhibited the efflux of RHO 123 from HK2 cells (Tramonti et al. 2001). Others authors, like Romiti et al, used the same protocol to demonstrate the functionality of P-gp, as well as the possibility of its modulation. These researchers, after an incubation with RHO 123 (5 μ g/mL) for 2 h, demonstrated that verapamil and cyclosporine A were, as in the previous study, P-gp inhibitors and cimetidine and trimethoprim did not cause any change in accumulation of RHO 123 inside the cell (Romiti et al. 2002). Chieli et al also first incubated HK2 cells at RHO 123 (5 μ g/mL) for 2 h and exposed them to the compounds to be studied by doing 3 washes with ice-cold Hank's buffer containing 20 μ M verapamil. However, they lysed the cells with 0.1% Triton X-100 to completely solubilize the intracellular RHO 123, to which the fluorescence intensity was measured (Chieli et al. 2009, 2012).

To our knowledge, there are no studies containing the compounds studied in the present study that carried out RHO 123 assays on HK2 cells. Even in other cells, no studies have

been found to test the ability of doxorubicin to activate/induce P-gp. However, some studies have shown the RIF-inducing role in other cell lines using this technique. Becquemont et al carried out a study analysing the lymphocyte P-gp expression and activity after rifampicin treatment (300 mg orally twice a day, for 3 days in a row). Various blood samples were made, being the last one drawn 12 h after the administration of the last dose of RIF. To test P-gp activity, lymphocytes were then incubated with RHO 123 (0.1 μ M, for 1 h at 37 °C), washed three times with ice-cold medium, and then transferred into dye-free medium for a further incubation in the presence or absence of 10 μ M verapamil, a P-gp inhibitor. They concluded that RIF does not induce P-gp expression in the studied cells, lymphocytes (Becquemont et al. 2000). Annaert et al, on the other hand, studied several possible modulators of P-gp, observing the *in vitro* disposition of rhodamine 123 (1 - 100 μ M), using sandwich-cultured rat hepatocytes. These cells were cultured in the presence of modulating agents, including verapamil (1 – 10 μ M), rifampicin (5 – 50 μ M), and dexamethasone (10 – 50 μ M), for 48 or 72 h. In the 48h RIF-treatment experiment, none of the inducers significantly affected RHO 123 accumulation; however, when this treatment was followed by a 24-h washout, RHO 123 accumulation increased up to 4-fold for one. In the 72 h treatment, 50 μ M rifampicin appeared to reduce RHO 123 intracellular accumulation (Annaert and Brouwer 2005). Kota et al analyzed P-gp expression, localization and function in the presence of rifampicin, in intestinal LS174T cells. To assess its functionality, cells were treated with RIF (10 μ M)/DMSO for 2 or 6 days, washed with PBS and then incubated with RHO 123 (10 μ M for 15 min), in the presence and absence of verapamil (10 μ M). Their results showed a 50% decrease in accumulated RHO 123 in intestinal LS174T cells after exposure with RIF for 48 h, which was reversed by verapamil, indicating that the decrease was P-gp-dependent (Kota et al. 2010). Vilas boas et al studied the inducing effect of a RIF derivative, 1,8-dibenzoyl-rifampicin (DiBenzRif) in an *in vitro* model of rat's BBB - RBE4 cells. An exposure to 5 μ M DiBenzRif was performed for 30 min or 24, 48 and 72 h, followed by HBSS washes (-/-), and an incubation in 2 μ M RHO 123 (30 min, at 37°C). These researchers also eliminated the possibility of MRP1 interference in RHO 123 transport by incubating RBE4 cells with RHO 123 and MK571 (MRP1 inhibitor). Thus, they obtained a significant increase in the intracellular RHO 123 content after DiBenzRif exposure for 30 min, 24 and 48 h, which seems to lose its intensity and significance with the increase in the incubation period (Vilas-Boas et al. 2013a). More recently, Hasanuzzaman et al analyzed the intracellular concentration of RHO 123 and prothionamide in the presence of RIF in THP1 macrophages. After RIF-treatment (100 μ M for 48 h), an incubation with RHO 123 (5 μ M) and cyclosporine A (20 μ M) was carried out for 90 min at 37°C. RIF-treatment significantly reduced the intracellular accumulation of RHO 123 and prothionamide,

compared to control macrophages, which was significantly suppressed by pregnane X receptor inhibitors resveratrol and ketoconazole (Hasanuzzaman et al. 2019).

On the other hand, there are also studies that prove the ability of xanthenes to activate/induce P-gp on other cell lines. Xanthenes scaffold effects on this pump expression and activity has been widely studied, including amino alkylthio xanthenes (Palmeira et al. 2012) and thioxanthonic derivatives. Silva et al studied five newly synthesized thioxanthonic derivatives as potential inducers of P-gp in Caco-2 cells. RHO 123 efflux was evaluated in the presence of the tested TXs (20 μ M) for 45 min, in order to evaluate immediate effects on P-gp activity as a result of a direct activation, and for 24 h, to analyze P-gp expression induced by the TXs. Using RHO 123 assays, all five thioxanthenes showed a significant increase in P-gp activity, when compared to control cells, in both conditions of the experiment. TX5 was the thioxanthone derivative that demonstrated the highest potential in inducing P-gp (Silva et al. 2015b). Rocha-Pereira evaluated the TX5 effects on P-gp expression/activity using Wistar Han rats. Their results showed that the efflux of RHO 123 (300 μ M) significantly increased in TX5-treated everted sacs from the distal portion of the rat ileum, when P-gp activity was evaluated in the presence of TX5 (20 μ M), an effect reversed by the P-gp inhibitor verapamil (100 μ M) (Rocha-Pereira et al. 2020). Lopes et al, on the other hand, studied the P-gp modulatory ability of new synthesized chiral aminated thioxanthenes in Caco-2 cells. Incubating simultaneously for 60 min all the tested compounds (20 μ M) with RHO 123, data demonstrated a significant decrease in the intracellular accumulation of the substrate, showing the increased efflux activity, when compared to control cells (Lopes et al. 2018).

As we have seen so far, HK2 cells have been used in several studies concerning P-gp, including its modulation. Nieri et al tested the possibility of endogenous and synthetic cannabinoid molecules to regulate P-gp activity on HK-2 cells. They showed, by Western Blotting, that P-gp activity can be inhibited by the endocannabinoid system and by synthetic cannabinoids in HK-2 cells, in a cannabinoid receptor (CB) 1 and CB2 independent pathway (Nieri et al. 2006). In this way, it would also be interesting from a future perspective to carry out Western Blotting assays to evaluate the expression of P-gp and its consequent increase in the presence of the possible studied inducers.

3.4. Cisplatin-induced cytotoxicity assays

Finally, some cytotoxicity studies were carried out to observe the existence of a reduction of cisplatin-induced nephrotoxicity caused by the studied compounds. As described in 2.6. **Cisplatin-induced cytotoxicity assays**, 3 assays with different exposure conditions were performed: 30 min of exposure to DOX, RIF, TX5 or ZOS (with further removal of the compounds before cisplatin exposure of 18 h); 30 and 48 h of exposure to DOX, RIF or TX5 (without removal of the compounds), plus 18 h of exposure to cisplatin. The results obtained in the 30-minute exposure tests are presented in Figure 20 and Figure 21.

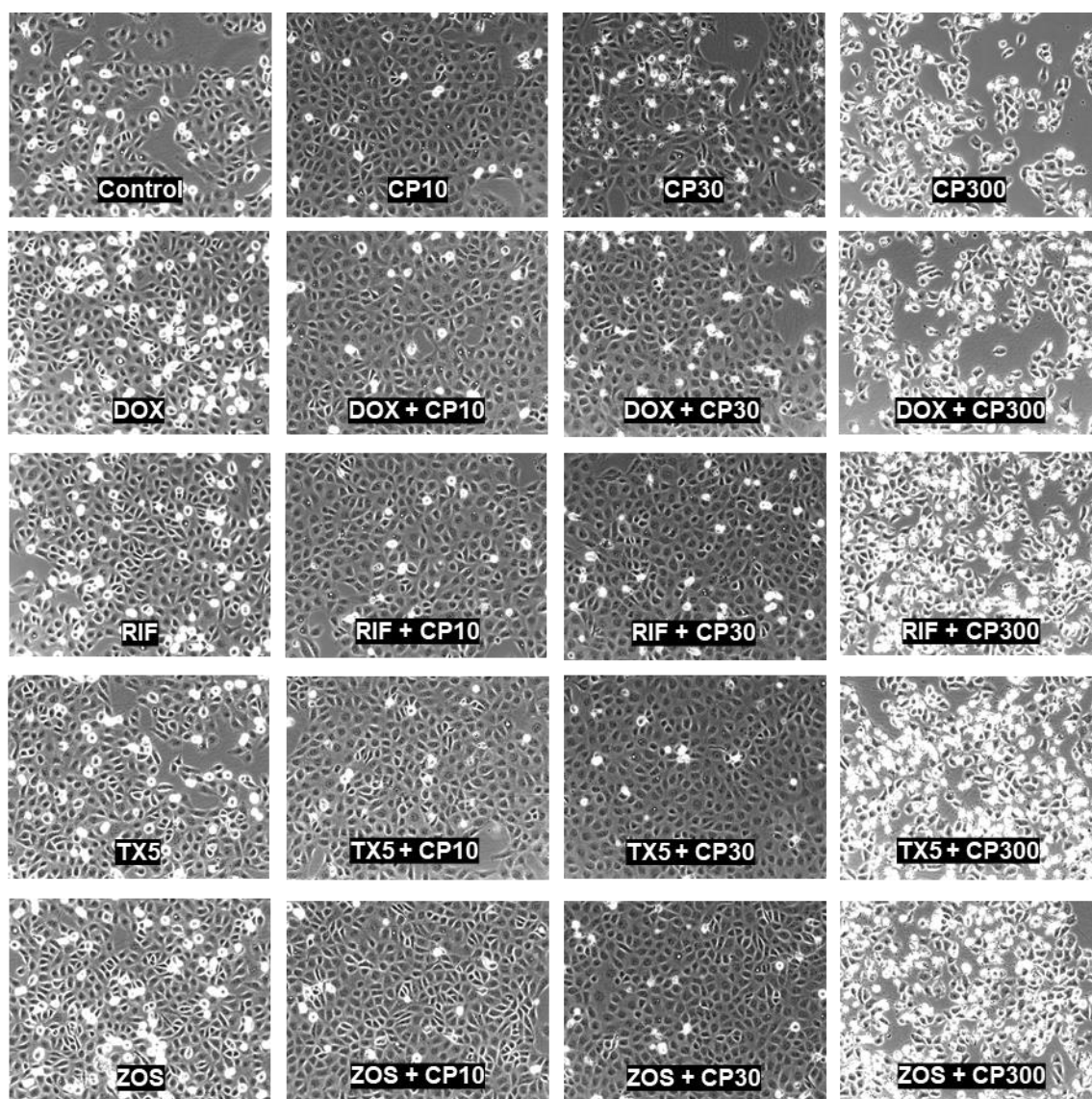


Figure 20. Photos obtained from an optic microscope in the HK2 cells exposed to doxorubicin (DOX; 2 μ M), rifampicin (RIF; 20 μ M), thioxanthone 5 (TX5; 20 μ M) or zosuquidar (ZOS; 1 μ M) for 30 min, plus 18 h exposed to cisplatin (CP; 10 μ M, 30 μ M and 300 μ M) in the cisplatin-induced cytotoxicity assay.

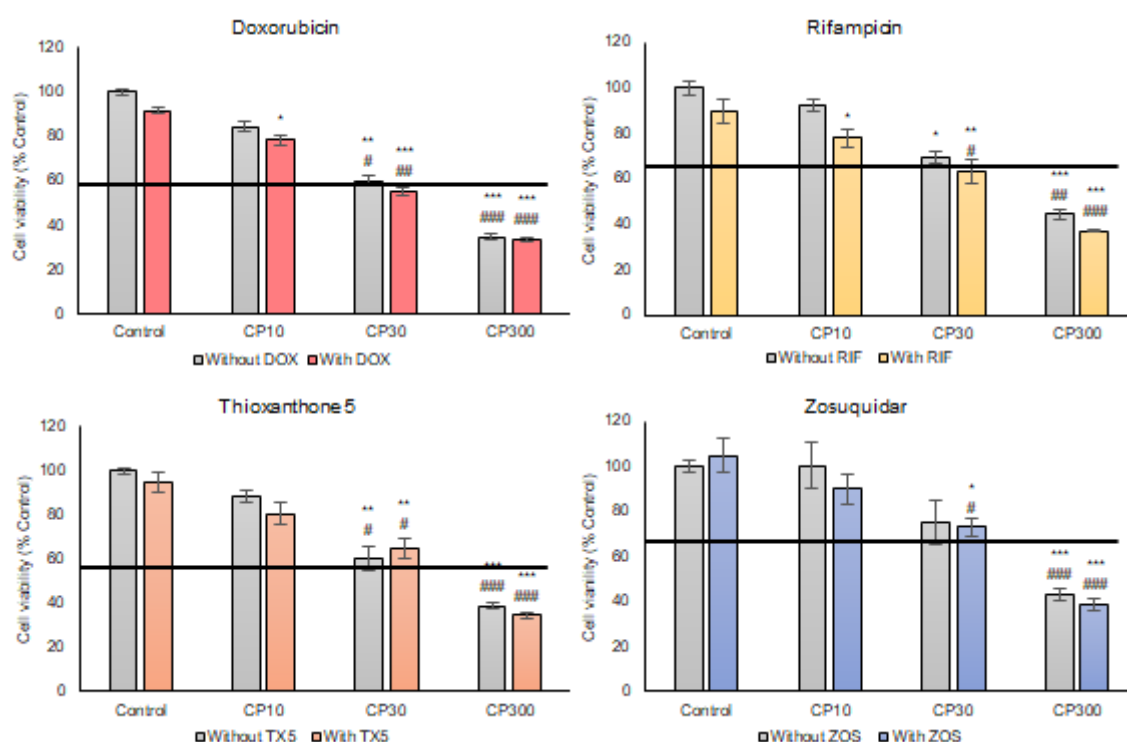


Figure 21. Cell viability (%) of HK2 cells exposed to doxorubicin (DOX; 2 μ M), rifampicin (RIF; 20 μ M), thioxanthone 5 (TX5; 20 μ M) and zosuquidar (ZOS; 1 μ M) for 30 min, in the cisplatin-induced cytotoxicity assays, based on the MTT assays. Data is presented as mean \pm standard error of 3 experiments with quadruplicates (n=12). Black line represents cell viability before treatment (Time 0). *: p<0.5, **: p<0.01, and ***: p<0.001, compared with control; #: p<0.05, ##: p<0.01, ###: p<0.001, compared with control with DOX, RIF, TX5 or ZOS.

According to these results, it was possible to observe that the compounds did not cause any type of protection against cisplatin. This may be due to the fact that, after 30 min of exposure, washes were made with PBS and thus the compounds were removed before exposure to cisplatin. In this way, cisplatin may have left the cells in the first hours of incubation, due to the increase of P-gp activity, but may have re-entered the cells after a few hours (since the incubation with cisplatin was 18 h), which makes us not see any significant changes caused by any of the compounds. One option would be to keep the compounds and simply add cisplatin to the respective wells. However, in this way, the cells would be exposed to the compounds for a total of 18.5 h, which would not reflect the mimicking conditions of the P-gp activation that is a faster process. Furthermore, to test the efficacy of the activation and the consequent protection against nephrotoxic agents, it will be better to use another *in vitro* model of cisplatin-induced cytotoxicity, or even another substance, in which the cells could be exposed to the toxic agent for a shorter period of time (probably at higher doses). Another limitation could be the low activation that we have seen in RHO 123 assays. Only TX5 has presented significantly changes in P-gp activity

(see **3.3. Evaluation of P-glycoprotein transport activity**), even it couldn't alter the cell viability in its presence.

The results obtained in the 48-hours exposure tests are presented in Figure 22 and Figure 23.

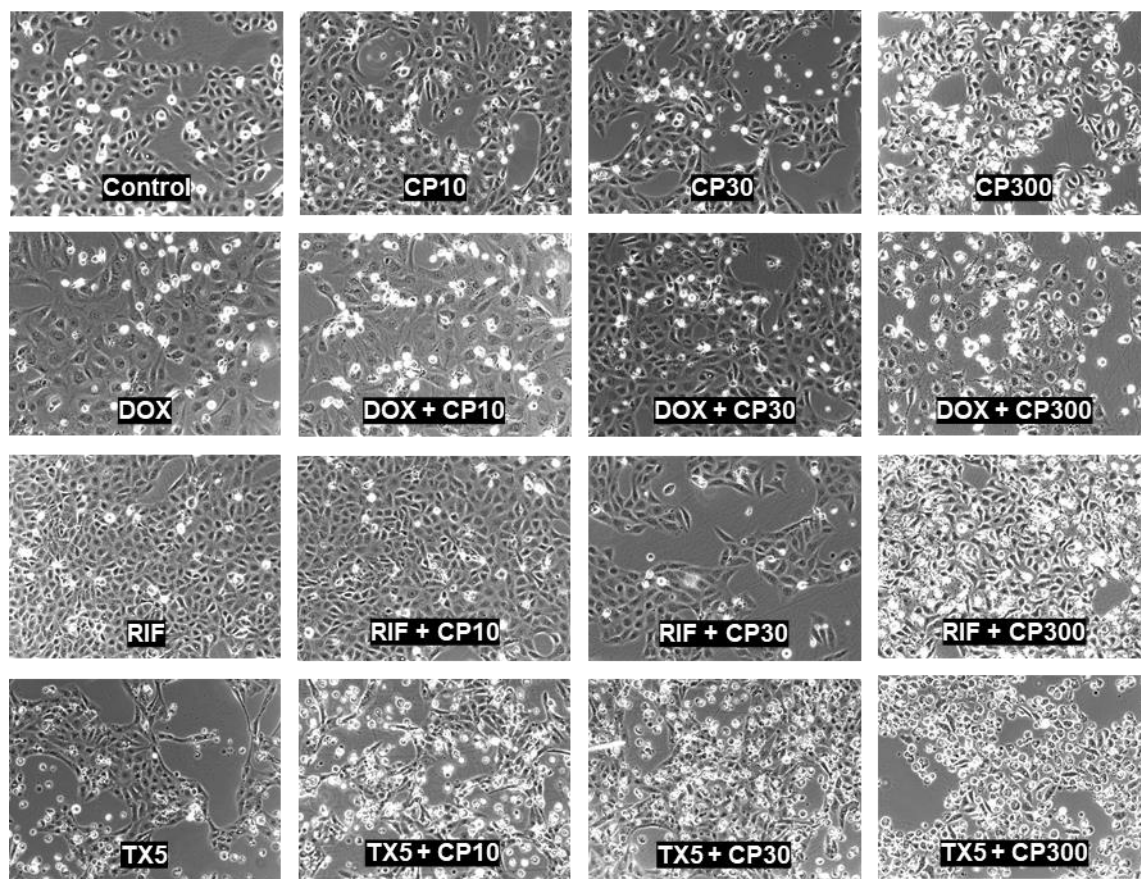


Figure 22. Photos obtained from an optic microscope in the HK2 cells exposed to doxorubicin (DOX; 2 μ M), rifampicin (RIF; 20 μ M) or thioxanthone 5 (TX5; 20 μ M) for 48 h, plus 18h exposed to cisplatin (CP; 10 μ M, 30 μ M and 300 μ M) in the cisplatin-induced cytotoxicity assay.

The results obtained in this test were different between the compounds. DOX and TX5 not only did not protect HK2 cells from cisplatin-induced cytotoxicity, but also showed some toxicity. This toxicity may be due to the fact that the cells are exposed to the compounds for a total of 66 h. Our cytotoxicity studies only contained exposure times up to 24 h, not revealing this toxicity induced by these compounds in longer times. On the other hand, a significant increase in cell viability was observed in the presence of RIF, for all studied cisplatin concentrations. However, comparing the cells exposed only to RIF with the control cells, it was observed that this compound has a proliferative effect. Thus, the increase in

cell viability observed in the presence of RIF may be caused by this proliferative effect and not, effectively, by its P-gp inducing effect that would decrease the intracellular concentration and cisplatin cytotoxicity in HK2 cells. Observing these results, it was decided to test a pre-exposure time of 30 h to DOX, RIF and TX5 plus 18 h of exposure to cisplatin (which results in a total of 48 h of exposure to these compounds).

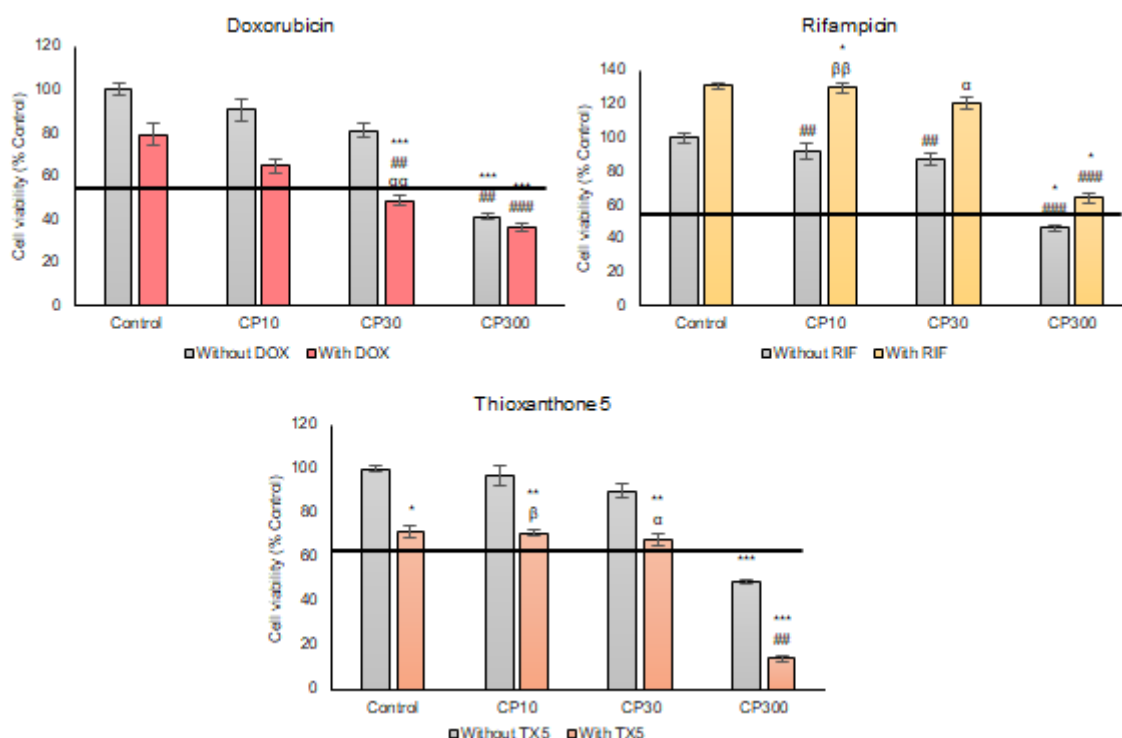


Figure 23. Cell viability (%) of HK2 cells exposed to doxorubicin (DOX; 2 μ M), rifampicin (RIF; 20 μ M), and thioxanthone 5 (TX5; 20 μ M), in the 48h cisplatin-induced cytotoxicity assays, based on the MTT assays. Data is presented as mean \pm standard error of 3 experiments with quadruplicates (n=12). Black line represents cell viability before treatment (Time 0). *: p<0.5, **: p<0.01, and ***: p<0.001, compared with control; ##: p<0.01, and ###: p<0.001, compared with control with DOX, RIF or TX5; β : p<0.05, $\beta\beta$: p<0.01, compared with CP10; α : p<0.05, compared with CP30.

The results obtained in the 30-hours exposure tests are presented in Figure 24, where it was possible to observe, again, different results for each of the tested compounds. DOX, once again, presented itself as a toxic compound for HK2 cells. Comparing the cells exposed only to DOX with the control cells, it was possible to see a significant difference, demonstrating in fact their toxic effect on these cells under these conditions. In addition, in HK2 cells exposed to DOX plus cisplatin, the toxic effect is even higher, further lowering their cell viability. This is probably caused by the long exposure time of exposure (48 h) that makes DOX a toxic compound to HK2 cells. Regarding RIF (20 μ M), under these

conditions, it is possible to observe an increase in the cell viability in its presence, reducing the toxic effect caused by cisplatin (10 μ M, 30 μ M and 300 μ M). However, a test with the addition of ZOS, the P-gp inhibitor, would be necessary in these wells to see if the RIF inducing effect would be suppressed, confirming that it is in fact the P-gp induction caused by RIF that is causing the decrease in cytotoxicity. It is still possible to observe a non-significant improvement in cell viability in the presence of TX5 in HK2 cells exposed to 10 μ M CP and 30 μ M CP, despite the toxicity that TX5 seems to present in these conditions (exposure of 48 h). However, in the future a 24 h exposure time should also be studied. In this way, it may be possible to observe a possible significant protection caused by DOX and TX5 against cisplatin cytotoxicity, since we predict that, under these conditions, these compounds will not have a toxic effect. On the other side, adjusting the experimental conditions, even RIF could present better results. According to these results, it is possible to conclude that the 30-hour exposure test showed the most reliable results and that, among the studied activators/inducers, RIF seems to have the best protective role against cisplatin-induced toxicity in HK2 cells.

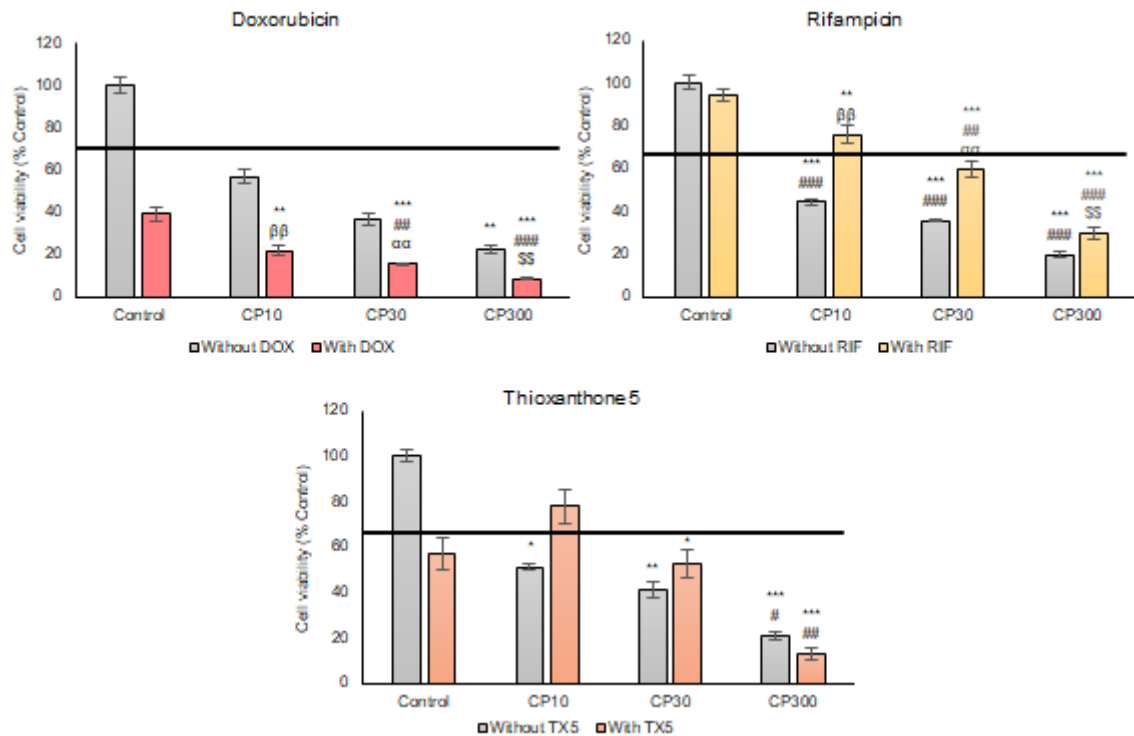


Figure 24. Cell viability (%) of HK2 cells exposed to doxorubicin (DOX; 2 μ M), rifampicin (RIF; 20 μ M), and thioxanthone 5 (TX5; 20 μ M), in the 30 + 18 h cisplatin-induced cytotoxicity assays, based on the MTT assays. Data is presented as mean \pm standard error of 3 experiments with quadruplicates (n=12). Black line represents cell viability before treatment (Time 0). *: p<0.5, **: p<0.01, and ***: p<0.001, compared with control with control; #: p<0.5, ##: p<0.01, and ###: p<0.001, compared with DOX, RIF or TX5; $\beta\beta$: p<0.01, compared with CP10; $\alpha\alpha$: p<0.01, compared with CP30; $\$ \$$: p<0.01, compared with CP300.

No studies were found in the literature that attempt to decrease cisplatin-induced cytotoxicity, in these conditions, using the doxorubicin, rifampicin or xanthenes (or its derivatives) in HK2 cells. Nonetheless, some studies have shown the effectiveness of these compounds in protecting against other nephrotoxic drugs in other cell lines.

Silva et al assessed doxorubicin ability to reduce paraquat cytotoxicity, in Caco-2 cells by MTT assay. This intestinal cell line was exposed to doxorubicin (0 – 5000 μ M, for 24 h), washed with PBS and, then, exposed to paraquat (0 – 5000 μ M, for 24 h). To confirm the involvement of P-gp in the DOX protective effects these incubations were repeated in the presence of a P-gp specific inhibitor for 30 min before DOX exposure. Their results suggested that P-gp induction with doxorubicin was effective in increasing P-gp expression and activity and, consequently, that P-gp induction by DOX protected the cells from PQ cytotoxicity (Silva et al. 2011). Silva et al evaluated paraquat cytotoxicity in Caco-2 cells by MTT assay, with and without incubation with DOX (final concentrations of 0, 10, 50 and 100 μ M, for 18 h), 6 h after PQ exposure (100 – 5000 μ M, final incubation period of 24 h). To confirm the involvement of P-gp in the DOX protective effects these incubations were repeated in the presence of a P-gp specific inhibitor for 30 min before DOX exposure. This group effectively observed an increase in PQ excretion from Caco-2 cells, resulting in less paraquat-induced cytotoxicity (Silva et al. 2013). Our data obtained on cells exposed to DOX are not in accordance with these articles; however, DOX had already been shown as a toxic agent for HK2 cells, which may explain the disparity of results in both cell lines (HK2 and Caco-2). On the other hand, in the present work, the toxic agent used was CP (and not PQ), which can also, together with DOX, decrease the cell viability of cells exposed to both.

Regarding RIF, there are also some studies that prove its important role in inducing P-gp and, consequently, in reducing cytotoxicity caused by nephrotoxic agents, which is in accordance with our data. Harmsen et al tested RIF ability to reduce toxicity caused by DOX (used in this article as a toxic agent under their conditions), using the LS180 cell line. A treatment with 10 μ M RIF was carried out for 72 h and, then, another one with DOX (serially diluted 0 – 20 μ M; dilution factor 2) for 48 h. Cell viability was assessed using a neutral red assay, showing that doxorubicin exposure cell viability was significantly higher in the rifampicin-treated cells, compared to the control cells (Harmsen et al. 2010). On the other hand, Vilas-Boas et al evaluated the effect of a RIF derivative - reduced rifampicin (RedRif) – on PQ-induced cytotoxicity. RBE4 cells were exposed to 10 μ M RedRif for 24, 48 and 72 h alone (preexposure) or simultaneously with growing concentrations of paraquat (0.5 - 50 μ M, for 48 h). The cytotoxicity evaluation was carried out by neutral red assay, showing that the simultaneous exposure to RedRif and paraquat during 48 h significantly

increased cell viability at 1, 5 and 10 μM paraquat. Significant protection from PQ-induced toxic effect at 15 μM paraquat was observed in the 24 and 48 h treatments. They also did another assay adding GF120918, a P-gp inhibitor, confirming the involvement of P-gp activity in RedRif protection of RBE4 cells against the PQ cytotoxicity (Vilas-Boas et al. 2013b).

Some studies have shown the protective effect of TXs against toxic agents in Caco-2 intestinal cells. Silva et al demonstrated a reduction in the cytotoxicity of PQ in the presence of thioxanthone derivatives, an effect which was reversed in the presence of the specific P-gp inhibitor, GF120918 (10.0 μM for TXs 1 – 5 and 20.0 μM for TX5). Paraquat cytotoxicity was evaluated in Caco-2 cells by the NR uptake assay, with and without simultaneous incubation with the tested TXs. Caco-2 cells were exposed to PQ (0 – 7500 μM) in the presence or absence of the TXs (20.0 μM) for 24 h. Their data have shown the potential of the thioxanthonic compounds in protecting against PQ-induced toxicity, especially TX5 which has been shown to have the greatest potential (Silva et al. 2015a). Silva et al, also by NR uptake assay, evaluated PQ (0 – 7500 μM , for 24 h) cytotoxicity in Caco-2 cells with and without simultaneous incubation with the tested xanthonones, X1 – X5 (20.0 μM), repeating the tests in the presence of a potent P-gp inhibitor, GF120918 (10.0 μM). The PQ cytotoxicity significantly decreased for the 500 – 5000 μM paraquat concentration range, which was significantly reversed in the presence of GF120918. This is, in the presence of this inhibitor, cell death increased significantly, demonstrating the involvement of dihydroxylated xanthonic derivatives in the induction of P-gp e, thus, in protection against its toxic substrates (Silva et al. 2014). These articles were not in accordance or against our data, since it was possible to observe just a tendency for TX5 to decrease cisplatin-induced nephrotoxicity in HK2 cells, although further studies and optimization of conditions are needed.

4. FINAL CONSIDERATIONS

P-glycoprotein (P-gp) is a transmembrane protein that acts as an efflux transporter of non-specific in various barrier sites, such as blood-brain barrier, liver, kidneys, among others. In the kidneys, this pump expels its various substrates from the renal proximal tubular cells into the urine, having a fundamental role in the detoxification of various xenobiotics. Thus, several investigators have been studying it and also the possibility of modeling it, which could be a possible therapeutic strategy since, for example, activating or inducing it will possibly eliminate more effectively toxic agents that tend to accumulate in renal proximal tubular cells, leading to a reduction in the nephrotoxicity caused by them.

Therefore, in this study, the possibility of activating/inducing P-gp in HK2 cells was studied, using DOX, RIF and TX5 as possible inducers/activators, through RHO 123 assays, a fluorescent substrate of P-gp. In addition, the possibility that these compounds reduced cisplatin (CP)-induced nephrotoxicity in HK2 cells was also evaluated, by MTT assays. Data obtained from RHO 123 assays in a short period, showed that TX5 was capable of activating P-gp, since HK2 cells exposed to that compound demonstrated a significant increase of the percentage of P-gp activity, when compared with the control cells. In a long period of time, results showed that all compounds increased P-gp activity. In addition, by MTT assays, cells exposed to CP (18 h) in presence or absence of RIF (added 30 h before the exposure to CP), showed that this compound was able to reduce the toxicity of the toxic agent, with a significant increase in cell viability in all the concentrations of CP applied to the HK2 cells. Data obtained from cells exposed to TX5 were promising, although there were no significant differences between cells exposed to TX5 (pre-exposure of 30 h) plus cisplatin (18 h) and cells exposed only to cisplatin (18 h).

In conclusion, it was possible to observe that, at least, one of the studied compounds, RIF, has a protective role against CP-induced cytotoxicity in HK2 cells. However, further studies are necessary in both tests to prove that the activation/induction of P-gp (in RHO 123 essays) and the reduction of cisplatin-induced cytotoxicity in the presence of these activators/inductors (in MTT assays) is due, effectively, to the involvement of P-gp and not by other processes. For this, both assays must be repeated in the presence of a specific P-gp inhibitor, zosuquidar, which must suppress the effects in P-gp described above, in HK2 cells. Therewithal, further studies should also be carried out to optimize the experimental conditions in order to demonstrate this protective role with DOX and TX5 (probably, with an exposure of 24 h) since both also showed potential in the activation and/or induction of P-gp.

5. REFERENCES

- Akamine Y, Yasui-Furukori N, Ieiri I, Uno T (2012) Psychotropic drug-drug interactions involving P-glycoprotein. *CNS Drugs* 26:959–973. <https://doi.org/10.1007/s40263-012-0008-z>
- Alam A, Kowal J, Broude E, et al (2019) Structural insight into substrate and inhibitor discrimination by human P-glycoprotein. *Science* 363:753–756. <https://doi.org/10.1126/science.aav7102>
- Alam A, Küng R, Kowal J, et al (2018) Structure of a zosuquidar and UIC2-bound human-mouse chimeric ABCB1. *Proc Natl Acad Sci U S A* 115:E1973–E1982. <https://doi.org/10.1073/pnas.1717044115>
- Aleksunes LM, Augustine LM, Scheffer GL, et al (2008) Renal xenobiotic transporters are differentially expressed in mice following cisplatin treatment. *Toxicology*. <https://doi.org/10.1016/j.tox.2008.06.009>
- Annaert PP, Brouwer KLR (2005) Assessment of drug interactions in hepatobiliary transport using rhodamine 123 in sandwich-cultured rat hepatocytes. *Drug Metab Dispos* 33:388–394. <https://doi.org/10.1124/dmd.104.001669>
- Anzai N, Jutabha P, Endou H (2010) Molecular mechanism of ochratoxin A transport in the kidney. *Toxins (Basel)* 2:1381–1398. <https://doi.org/10.3390/toxins2061381>
- Arakawa H, Kubo H, Washio I, et al (2019) Rat Kidney Slices for Evaluation of Apical Membrane Transporters in Proximal Tubular Cells. *J Pharm Sci* 108:2798–2804. <https://doi.org/10.1016/j.xphs.2019.03.031>
- Arany I, Safirstein RL (2003) Cisplatin nephrotoxicity. *Semin Nephrol* 23:460–464. [https://doi.org/10.1016/S0270-9295\(03\)00089-5](https://doi.org/10.1016/S0270-9295(03)00089-5)
- Balayssac D, Authier N, Cayre A, Coudore F (2005) Does inhibition of P-glycoprotein lead to drug-drug interactions? *Toxicol Lett* 156:319–329. <https://doi.org/10.1016/j.toxlet.2004.12.008>
- Becquemont L, Camus M, Eschwege V, et al (2000) Lymphocyte P-glycoprotein expression and activity before and after rifampicin in man. *Fundam Clin Pharmacol* 14:519–525. <https://doi.org/10.1111/j.1472-8206.2000.tb00435.x>

- Brown CDA, Sayer R, Windass AS, et al (2008) Characterisation of human tubular cell monolayers as a model of proximal tubular xenobiotic handling. *Toxicol Appl Pharmacol* 233:428–438. <https://doi.org/10.1016/J.TAAP.2008.09.018>
- Bush KT, Wu W, Lun C, Nigam SK (2017) The drug transporter OAT3 (SLC22A8) and endogenous metabolite communication via the gut–liver– kidney axis. *J Biol Chem* 292:15789–15803. <https://doi.org/10.1074/jbc.M117.796516>
- Callaghan R, Luk F, Bebawy M (2014) Inhibition of the Multidrug Resistance P-Glycoprotein: Time for a Change of Strategy? *Drug Metab Dispos* 42:623–631. <https://doi.org/10.1124/dmd.113.056176>
- Cárdenas-González M, Jacobo Estrada T, Rodríguez-Muñoz R, et al (2016) Sub-chronic exposure to fluoride impacts the response to a subsequent nephrotoxic treatment with gentamicin. *J Appl Toxicol* 36:309–319. <https://doi.org/10.1002/jat.3186>
- Cascorbi I (2011) P-glycoprotein: Tissue Distribution, Substrates, and Functional Consequences of Genetic Variations. In: *Handbook of Experimental Pharmacology*. pp 261–283
- Chen M, Yin H, Bai P, et al (2016) ABC transporters affect the elimination and toxicity of CdTe quantum dots in liver and kidney cells. *Toxicol Appl Pharmacol* 303:11–20. <https://doi.org/10.1016/j.taap.2016.04.017>
- Chen Y, Zhang S, Sorani M, Giacomini KM (2007) Transport of paraquat by human organic cation transporters and multidrug and toxic compound extrusion family. *J Pharmacol Exp Ther* 322:695–700. <https://doi.org/10.1124/jpet.107.123554>
- Chieli E, Romiti N, Catiana Zampini I, et al (2012) Effects of *Zuccagnia punctata* extracts and their flavonoids on the function and expression of ABCB1/P-glycoprotein multidrug transporter. *J Ethnopharmacol* 144:797–801. <https://doi.org/10.1016/j.jep.2012.10.012>
- Chieli E, Romiti N, Rodeiro I, Garrido G (2009) In vitro effects of *Mangifera indica* and polyphenols derived on ABCB1/P-glycoprotein activity. *Food Chem Toxicol* 47:2703–2710. <https://doi.org/10.1016/j.fct.2009.07.017>
- Chow ECY, Durk MR, Cummins CL, Pang KS (2011) 1 α ,25-dihydroxyvitamin D3 up-regulates P-glycoprotein via the vitamin D receptor and not farnesoid X receptor in both *fxr*(-/-) and *fxr*(+/+) mice and increased renal and brain efflux of digoxin in mice in vivo. *J Pharmacol Exp Ther* 337:846–859. <https://doi.org/10.1124/jpet.111.179101>

- Chufan EE, Kapoor K, Ambudkar S V (2016) Drug-protein hydrogen bonds govern the inhibition of the ATP hydrolysis of the multidrug transporter P-glycoprotein. *Biochem Pharmacol* 101:40–53. <https://doi.org/10.1016/j.bcp.2015.12.007>
- Crona DJ, Faso A, Nishijima TF, et al (2017) A Systematic Review of Strategies to Prevent Cisplatin-Induced Nephrotoxicity. *Oncologist* 22:609–619. <https://doi.org/10.1634/theoncologist.2016-0319>
- DeGorter MK, Xia CQ, Yang JJ, Kim RB (2012) Drug Transporters in Drug Efficacy and Toxicity. *Annu Rev Pharmacol Toxicol* 52:249–273. <https://doi.org/10.1146/annurev-pharmtox-010611-134529>
- Döring B, Petzinger E (2014) Phase 0 and phase III transport in various organs: Combined concept of phases in xenobiotic transport and metabolism. *Drug Metab Rev* 46:261–282. <https://doi.org/10.3109/03602532.2014.882353>
- Elmeliegy M, Láng I, Smolyarchuk EA, et al (2020a) Evaluation of the effect of P-glycoprotein inhibition and induction on talazoparib disposition in patients with advanced solid tumours. *Br J Clin Pharmacol* 86:771–778. <https://doi.org/10.1111/bcp.14178>
- Elmeliegy M, Vourvahis M, Guo C, Wang DD (2020b) Effect of P-glycoprotein (P-gp) Inducers on Exposure of P-gp Substrates: Review of Clinical Drug–Drug Interaction Studies. *Clin Pharmacokinet*. <https://doi.org/10.1007/s40262-020-00867-1>
- Elyasi S, Khalili H, Dashti-Khavidaki S, Mohammadpour A (2012) Vancomycin-induced nephrotoxicity: Mechanism, incidence, risk factors and special populations. A literature review. *Eur J Clin Pharmacol* 68:1243–1255. <https://doi.org/10.1007/s00228-012-1259-9>
- Galvao J, Davis B, Tilley M, et al (2014) Unexpected low-dose toxicity of the universal solvent DMSO. *FASEB J* 28:1317–1330. <https://doi.org/10.1096/fj.13-235440>
- Gameiro M, Silva R, Rocha-Pereira C, et al (2017) Cellular models and in vitro assays for the screening of modulators of P-gp, MRP1 and BCRP. *Molecules* 22:4–6. <https://doi.org/10.3390/molecules22040600>
- Genchi G, Sinicropi MS, Carocci A, et al (2017) Mercury exposure and heart diseases. *Int J Environ Res Public Health* 14:1–13. <https://doi.org/10.3390/ijerph14010074>

- George B, You D, Joy MS, Aleksunes LM (2017) Xenobiotic transporters and kidney injury. *Adv Drug Deliv Rev* 116:73–91. <https://doi.org/10.1016/j.addr.2017.01.005>
- Giacomini K, Huang S, Tweedie D, et al (2010) Membrane Transporters in Drug Development. 1–42. <https://doi.org/10.1016/B978-0-12-398339-8.00001-X>
- Giacomini KM, Huang S-M (2013) Transporters in Drug Development and Clinical Pharmacology. *Clin Pharmacol Ther* 94:3–9. <https://doi.org/10.1038/clpt.2013.86>
- Gil-Martins E, Barbosa DJ, Silva V, et al (2020) Dysfunction of ABC transporters at the blood-brain barrier: Role in neurological disorders. *Pharmacol Ther* 213:107554. <https://doi.org/10.1016/j.pharmthera.2020.107554>
- Gomez-Zepeda D, Taghi M, Smirnova M, et al (2019) LC–MS/MS-based quantification of efflux transporter proteins at the BBB. *J Pharm Biomed Anal* 164:496–508. <https://doi.org/10.1016/j.jpba.2018.11.013>
- Grobbelaar M, Louw GE, Sampson SL, et al (2019) Evolution of rifampicin treatment for tuberculosis. *Infect Genet Evol* 74:103937. <https://doi.org/10.1016/j.meegid.2019.103937>
- Harmsen S, Meijerman I, Febus CL, et al (2010) PXR-mediated induction of P-glycoprotein by anticancer drugs in a human colon adenocarcinoma-derived cell line. *Cancer Chemother Pharmacol* 66:765–771. <https://doi.org/10.1007/s00280-009-1221-4>
- Harrach S, Ciarimboli G (2015) Role of transporters in the distribution of platinum-based drugs. *Front Pharmacol* 6:1–7. <https://doi.org/10.3389/fphar.2015.00085>
- Hasanuzzaman M, Yi M, Cho M, et al (2019) Rifampin Induces Expression of P-glycoprotein on the THP1 Cell-Derived Macrophages, Causing Decrease Intramacrophage Concentration of Prothionamide. *J Pharm Sci* 108:3106–3111. <https://doi.org/10.1016/j.xphs.2019.04.009>
- Hoffmeyer S, Burk O, Von Richter O, et al (2000) Functional polymorphisms of the human multidrug-resistance gene: Multiple sequence variations and correlation of one allele with P-glycoprotein expression and activity in vivo. *Proc Natl Acad Sci U S A* 97:3473–3478. <https://doi.org/10.1073/pnas.97.7.3473>
- Huerta C, Varas-Lorenzo C, Castellsague J, García Rodríguez LA (2006) Non-steroidal anti-inflammatory drugs and risk of first hospital admission for heart failure in the

- general population. *Heart* 92:1610–1615. <https://doi.org/10.1136/hrt.2005.082388>
- Huo X, Liu K (2018) Renal organic anion transporters in drug–drug interactions and diseases. *Eur J Pharm Sci* 112:8–19. <https://doi.org/10.1016/j.ejps.2017.11.001>
- Iqbal T, Kinjo M, Dowling TC (2005) Determination of Rhodamine 123 in cell lysate by HPLC with visible wavelength detection. *J Chromatogr B Anal Technol Biomed Life Sci* 814:259–262. <https://doi.org/10.1016/j.jchromb.2004.10.037>
- Ivanyuk A, Livio F, Biollaz J, Buclin T (2017) Renal Drug Transporters and Drug Interactions. *Clin Pharmacokinet* 56:825–892. <https://doi.org/10.1007/s40262-017-0506-8>
- Jenkinson SE, Chung GW, van Loon E, et al (2012) The limitations of renal epithelial cell line HK-2 as a model of drug transporter expression and function in the proximal tubule. *Pflugers Arch* 464:601–611. <https://doi.org/10.1007/s00424-012-1163-2>
- Juliano RL, Ling V (1976) A surface glycoprotein modulating drug permeability in Chinese hamster ovary cell mutants. *BBA - Biomembr* 455:152–162. [https://doi.org/10.1016/0005-2736\(76\)90160-7](https://doi.org/10.1016/0005-2736(76)90160-7)
- Karasawa T, Steyger PS (2015) An integrated view of cisplatin-induced nephrotoxicity and ototoxicity. *Toxicol Lett* 237:219–227. <https://doi.org/10.1016/j.toxlet.2015.06.012>
- Kim RB (2002) Drugs as P-glycoprotein substrates , inhibitors , and inducers . *Publication Types , MeSH Terms , Substances , Grant Support*. 34:11996011
- Kim RB, Leake BF, Choo EF, et al (2001) Identification of functionally variant MDR1 alleles among European Americans and African Americans. *Clin Pharmacol Ther* 70:189–199. <https://doi.org/10.1067/mcp.2001.117412>
- Klaassen CD, Lu H (2008) Xenobiotic Transporters: Ascribing Function from Gene Knockout and Mutation Studies. *Toxicol Sci* 101:186–196. <https://doi.org/10.1093/toxsci/kfm214>
- Konieczna A, Erdösová B, Lichnovská R, et al (2011) Differential expression of ABC transporters (MDR1, MRP1, BCRP) in developing human embryos. *J Mol Histol* 42:567–574. <https://doi.org/10.1007/s10735-011-9363-1>
- König J, Müller F, Fromm MF (2013) Transporters and Drug-Drug Interactions: Important Determinants of Drug Disposition and Effects. *Pharmacol Rev* 65:944–966.

<https://doi.org/10.1124/pr.113.007518>

- Kota BP, Tran VH, Allen J, et al (2010) Characterization of PXR mediated P-glycoprotein regulation in intestinal LS174T cells. *Pharmacol Res* 62:426–431. <https://doi.org/10.1016/j.phrs.2010.07.001>
- Kotowski MJ, Bogacz A, Bartkowiak-Wieczorek J, et al (2019) Effect of Multidrug-Resistant 1 (MDR1) and CYP3A4*1B Polymorphisms on Cyclosporine-Based Immunosuppressive Therapy in Renal Transplant Patients. *Ann Transplant* 24:108–114. <https://doi.org/10.12659/AOT.914683>
- Kumar P de T-P pd., Nagarajan A, Uchil PD (2018) Analysis of Cell Viability by the MTT Assay. *Cold Spring Harb Protoc* 2018:. <https://doi.org/10.1101/pdb.prot095505>
- Lash H (2019) Environmental and Genetic Factors Influencing Kidney Toxicity. *Semin Nephrol* 39:132–140. <https://doi.org/10.1016/j.semnephrol.2018.12.003>
- Leopoldo M, Nardulli P, Contino M, et al (2019) An updated patent review on P-glycoprotein inhibitors (2011-2018). *Expert Opin Ther Pat* 29:455–461. <https://doi.org/10.1080/13543776.2019.1618273>
- Liu HC, Jamshidi N, Chen Y, et al (2016) An organic anion transporter 1 (oat1)-centered metabolic network. *J Biol Chem* 291:19474–19486. <https://doi.org/10.1074/jbc.M116.745216>
- Lopes A, Martins E, Silva R, et al (2018) Chiral Thioxanthenes as Modulators of P-glycoprotein: Synthesis and Enantioselectivity Studies. *Molecules* 23:. <https://doi.org/10.3390/molecules23030626>
- Lopez-Novoa JM, Quiros Y, Vicente L, et al (2011) New insights into the mechanism of aminoglycoside nephrotoxicity: An integrative point of view. *Kidney Int* 79:33–45. <https://doi.org/10.1038/ki.2010.337>
- Manohar S, Leung N (2017) Cisplatin nephrotoxicity : a review of the literature. *J Nephrol* 0:0. <https://doi.org/10.1007/s40620-017-0392-z>
- Martins E, Silva V, Lemos A, et al (2019) Newly synthesized oxygenated xanthenes as potential P-glycoprotein activators: In vitro, ex vivo, and in silico studies. *Molecules* 24:. <https://doi.org/10.3390/molecules24040707>

- Masereeuw R, Heemskerk S, Peters JGP, et al (2010) Regulation of P-glycoprotein in renal proximal tubule epithelial cells by LPS and TNF- α . *J Biomed Biotechnol* 2010:. <https://doi.org/10.1155/2010/525180>
- Mollazadeh S, Sahebkar A, Hadizadeh F, et al (2018) Structural and functional aspects of P-glycoprotein and its inhibitors. *Life Sci* 214:118–123. <https://doi.org/10.1016/j.lfs.2018.10.048>
- Momper JD, Yang J, Gockenbach M, et al (2019) Dynamics of Organic Anion Transporter-Mediated Tubular Secretion during Postnatal Human Kidney Development and Maturation. *Clin J Am Soc Nephrol* 14:540–548. <https://doi.org/10.2215/CJN.10350818>
- Nieri P, Romiti N, Adinolfi B, et al (2006) Modulation of P-glycoprotein activity by cannabinoid molecules in HK-2 renal cells. *Br J Pharmacol* 148:682–687. <https://doi.org/10.1038/sj.bjp.0706778>
- Nies AT, Herrmann E, Brom M, Keppler D (2008) Vectorial transport of the plant alkaloid berberine by double-transfected cells expressing the human organic cation transporter 1 (OCT1, SLC22A1) and the efflux pump MDR1 P-glycoprotein (ABCB1). *Naunyn Schmiedeberg's Arch Pharmacol* 376:449–461. <https://doi.org/10.1007/s00210-007-0219-x>
- Nigam SK, Bush KT, Martovetsky G, et al (2014) The Organic Anion Transporter (OAT) Family: A Systems Biology Perspective. *Physiol Rev* 95:83–123. <https://doi.org/10.1152/physrev.00025.2013>
- Nolin TD, Himmelfarb J (2010) Mechanisms of Drug-Induced Nephrotoxicity. In: *Handbook of Experimental Pharmacology*. pp 111–130
- Orr SE, Bridges CC (2017) Chronic Kidney Disease and Exposure to Nephrotoxic Metals. *Int J Mol Sci* 18:1039. <https://doi.org/10.3390/ijms18051039>
- Palmeira A, Vasconcelos MH, Paiva A, et al (2012) Dual inhibitors of P-glycoprotein and tumor cell growth: (Re)discovering thioxanthenes. *Biochem Pharmacol* 83:57–68. <https://doi.org/10.1016/j.bcp.2011.10.004>
- Park EJ, Kwon HK, Choi YM, et al (2012) Doxorubicin Induces Cytotoxicity through Upregulation of pERK-Dependent ATF3. *PLoS One* 7:2–11. <https://doi.org/10.1371/journal.pone.0044990>

- Pugazhendhi A, Edison TNJI, Velmurugan BK, et al (2018) Toxicity of Doxorubicin (Dox) to different experimental organ systems. *Life Sci* 200:26–30. <https://doi.org/10.1016/j.lfs.2018.03.023>
- Quadri JA, Sarwar S, Sinha A, et al (2018) Fluoride-associated ultrastructural changes and apoptosis in human renal tubule: a pilot study. *Hum Exp Toxicol* 37:1199–1206. <https://doi.org/10.1177/0960327118755257>
- Radi ZA (2019) Kidney Pathophysiology, Toxicology, and Drug-Induced Injury in Drug Development. *Int J Toxicol*. <https://doi.org/10.1177/1091581819831701>
- Ramalakshmi S, Bastacky S, Johnson JP (2003) Levofloxacin-induced granulomatous interstitial nephritis. *Am J Kidney Dis* 41:e7.1-e7.5. <https://doi.org/10.1053/ajkd.2003.50064>
- Ranzani GN, De Gregori S, De Gregori M, et al (2009) Interindividual variability of drug transporters: Impact on opioid treatment in chronic renal failure. *Eur J Pain Suppl* 3:21–28. <https://doi.org/10.1016/j.eujps.2009.07.010>
- Robertson EE, Rankin GO (2006) Human renal organic anion transporters: Characteristics and contributions to drug and drug metabolite excretion. *Pharmacol Ther* 109:399–412. <https://doi.org/10.1016/j.pharmthera.2005.07.005>
- Rocha-Pereira C, Ghanem CI, Silva R, et al (2020) P-glycoprotein activation by 1-(propan-2-ylamino)-4-propoxy-9H-thioxanthen-9-one (TX5) in rat distal ileum: ex vivo and in vivo studies. *Toxicol Appl Pharmacol* 386:114832. <https://doi.org/10.1016/j.taap.2019.114832>
- Romiti N, Tramonti G, Chieli E (2002) Influence of Different Chemicals on MDR-1 P-Glycoprotein Expression and Activity in the HK-2 Proximal Tubular Cell Line. *Toxicol Appl Pharmacol* 183:83–91. <https://doi.org/10.1006/taap.2002.9461>
- Saiz-Rodríguez M, Belmonte C, Román M, et al (2018) Effect of ABCB1 C3435T Polymorphism on Pharmacokinetics of Antipsychotics and Antidepressants. *Basic Clin Pharmacol Toxicol* 123:474–485. <https://doi.org/10.1111/bcpt.13031>
- Sancho-Martínez SM, Piedrafita FJ, Cannata-Andía JB, et al (2011) Necrotic concentrations of cisplatin activate the apoptotic machinery but inhibit effector caspases and interfere with the execution of apoptosis. *Toxicol Sci* 122:73–85. <https://doi.org/10.1093/toxsci/kfr098>

- Sancho-Martínez SM, Prieto-García L, Prieto M, et al (2018) N -acetylcysteine transforms necrosis into apoptosis and affords tailored protection from cisplatin cytotoxicity. *Toxicol Appl Pharmacol* 349:83–93. <https://doi.org/10.1016/j.taap.2018.04.010>
- Schlessinger A, Khuri N, Giacomini KM, Sali A (2013) Molecular modeling and ligand docking for solute carrier (SLC) transporters. *Curr Top Med Chem.* <https://doi.org/10.2174/1568026611313070007>
- Semeniuk M, Ceré LI, Ciriaci N, et al (2020) Regulation of hepatic P-gp expression and activity by genistein in rats. *Arch Toxicol* 94:1625–1635. <https://doi.org/10.1007/s00204-020-02708-3>
- Shen H, Scialis RJ, Lehman-McKeeman L (2019) Xenobiotic Transporters in the Kidney: Function and Role in Toxicity. *Semin Nephrol* 39:159–175. <https://doi.org/10.1016/j.semnephrol.2018.12.010>
- Shi M, McMillan KL, Wu J, et al (2018) Cisplatin nephrotoxicity as a model of chronic kidney disease. *Lab Invest* 98:1105–1121. <https://doi.org/10.1038/s41374-018-0063-2>
- Silva R, Carmo H, Dinis-Oliveira R, et al (2011) In vitro study of P-glycoprotein induction as an antidotal pathway to prevent cytotoxicity in Caco-2 cells. *Arch Toxicol* 85:315–326. <https://doi.org/10.1007/s00204-010-0587-8>
- Silva R, Carmo H, Vilas-Boas V, et al (2013) Doxorubicin decreases paraquat accumulation and toxicity in Caco-2 cells. *Toxicol Lett* 217:34–41. <https://doi.org/10.1016/j.toxlet.2012.11.028>
- Silva R, Palmeira A, Carmo H, et al (2015a) P-glycoprotein induction in Caco-2 cells by newly synthesized thioxanthenes prevents paraquat cytotoxicity. *Arch Toxicol* 89:1783–1800. <https://doi.org/10.1007/s00204-014-1333-4>
- Silva R, Sousa E, Carmo H, et al (2014) Induction and activation of P-glycoprotein by dihydroxylated xanthenes protect against the cytotoxicity of the P-glycoprotein substrate paraquat. *Arch Toxicol* 88:937–951. <https://doi.org/10.1007/s00204-014-1193-y>
- Silva R, Vilas-boas V, Carmo H, et al (2015b) Pharmacology & Therapeutics Modulation of P-glycoprotein efflux pump: induction and activation as a therapeutic strategy. *Pharmacol Ther* 149:1–123. <https://doi.org/10.1016/j.pharmthera.2014.11.013>

- Silva V, Gil-Martins E, Rocha-Pereira C, et al (2020) Oxygenated xanthenes as P-glycoprotein modulators at the intestinal barrier: in vitro and docking studies. *Med Chem Res* 29:1041–1057. <https://doi.org/10.1007/s00044-020-02544-1>
- Su Z, Ye J, Qin Z, Ding X (2015) Protective effects of madecassoside against Doxorubicin induced nephrotoxicity in vivo and in vitro. *Sci Rep* 5:1–14. <https://doi.org/10.1038/srep18314>
- Tramonti G, Romiti N, Norpoth M, Chieli E (2001) P-glycoprotein in HK-2 proximal tubule cell line. *Ren Fail* 23:331–337. <https://doi.org/10.1081/JDI-100104717>
- Uchida Y, Toyohara T, Ohtsuki S, et al (2016) Quantitative Targeted Absolute Proteomics for 28 Transporters in Brush-Border and Basolateral Membrane Fractions of Rat Kidney. *J Pharm Sci* 105:1011–1016. <https://doi.org/10.1002/jps.24645>
- Veiga-Matos J, Remião F, Morales AI (2020) Pharmacokinetics and Toxicokinetics Roles of Membrane Transporters at Kidney Level. *J Pharm Pharm Sci* 23:333–356. <https://doi.org/10.18433/jpps30865>
- Vilas-Boas V, Silva R, Nunes C, et al (2013a) Mechanisms of P-gp inhibition and effects on membrane fluidity of a new rifampicin derivative, 1,8-dibenzoyl-rifampicin. *Toxicol Lett* 220:259–266. <https://doi.org/10.1016/j.toxlet.2013.05.005>
- Vilas-Boas V, Silva R, Palmeira A, et al (2013b) Development of Novel Rifampicin-Derived P-Glycoprotein Activators/Inducers. Synthesis, In Silico Analysis and Application in the RBE4 Cell Model, Using Paraquat as Substrate. *PLoS One* 8:1–13. <https://doi.org/10.1371/journal.pone.0074425>
- Volarevic V, Djokovic B, Jankovic MG, et al (2019) Molecular mechanisms of cisplatin-induced nephrotoxicity: a balance on the knife edge between renoprotection and tumor toxicity. *J Biomed Sci* 26:25. <https://doi.org/10.1186/s12929-019-0518-9>
- Vormann MK, Gijzen L, Hutter S, et al (2018) Nephrotoxicity and Kidney Transport Assessment on 3D Perfused Proximal Tubules. *AAPS J* 20:90. <https://doi.org/10.1208/s12248-018-0248-z>
- Waghray D, Zhang Q (2018) Inhibit or Evade Multidrug Resistance P-Glycoprotein in Cancer Treatment. *J Med Chem* 61:5108–5121. <https://doi.org/10.1021/acs.jmedchem.7b01457>

- Wang L, Zhang L, Liu F, Sun Y (2019) Molecular Energetics of Doxorubicin Pumping by Human P-Glycoprotein. *J Chem Inf Model* 59:3889–3898. <https://doi.org/10.1021/acs.jcim.9b00429>
- Wang Z, Lin YS, Dickmann LJ, et al (2013) Enhancement of hepatic 4-hydroxylation of 25-hydroxyvitamin D 3 through CYP3A4 induction in vitro and in vivo: Implications for drug-induced osteomalacia. *J Bone Miner Res* 28:1101–1116. <https://doi.org/10.1002/jbmr.1839>
- Wessler JD, Grip LT, Mendell J, Giugliano RP (2013) The P-glycoprotein transport system and cardiovascular drugs. *J Am Coll Cardiol* 61:2495–2502. <https://doi.org/10.1016/j.jacc.2013.02.058>
- Wu J, Lin N, Li F, et al (2016) Induction of P-glycoprotein expression and activity by Aconitum alkaloids: Implication for clinical drug-drug interactions. *Sci Rep* 6:1–12. <https://doi.org/10.1038/srep25343>
- Yin J, Wang J (2016) Renal drug transporters and their significance in drug-drug interactions. *Acta Pharm Sin B* 6:363–373. <https://doi.org/10.1016/j.apsb.2016.07.013>
- Zhang Q, Wu G, Guo S, et al (2020) Effects of tristetraprolin on doxorubicin (adriamycin)-induced experimental kidney injury through inhibiting IL-13/STAT6 signal pathway. *Am J Transl Res* 12:1203–1221
- Zhou Y, Yang Y, Wang P, et al (2019) Adefovir accumulation and nephrotoxicity in renal interstitium: Role of organic anion transporters of kidney. *Life Sci* 224:41–50. <https://doi.org/10.1016/j.lfs.2019.03.042>